Charles University

Faculty of Medicine in Pilsen

Department of Stomatology

Biocompatibility of Implantable Materials

Focused on Titanium Dental Implants

Biokompatibilita implantabilních materialů

se zaměřením na titanové dentální implantáty

Dissertation Thesis

MDDr. Amin Moztarzadeh

Supervisor: Ing. Václav Babuška, Ph.D.

Pilsen 2017

Acknowledgments

I am using this opportunity to express my gratitude to everyone who supported and helped me throughout my doctoral studies.

In the very first place, my appreciation belongs to the supervisor of my postgraduate studies, Ing. Václav Babuška, Ph.D., for his valuable scientific guidance, advice and patience; and the whole team of Department of Medical Chemistry and Biochemistry (Faculty of Medicine in Pilsen).

Furthermore, I would like to thank the Head of Department of Stomatology of Faculty Hospital in Pilsen, doc. MUDr. Antonín Zicha, CSc., for providing me the possibility to enter the Ph.D. programme and for his support during the whole period of my studies.

Finally, I would like to thank to my wife, MDDr. Jana Moztarzadeh, and my brother, MUDr. Omid Moztarzadeh, Ph.D., for their moral support and understanding during all these years.

Declaration

I declare that this thesis has been composed solely by myself and all sources used within this work are cited inside.

This work has not been submitted, in whole or in part, in any previous application for a degree.

MDDr. Amin Moztarzadeh

Date: ……..

Signature: ……..

Abstract

This dissertation thesis deals with the evaluation of biocompatibility and osseointegration of nanostructured titanium materials used for dental implants. Bulk material topography and surface modification of titanium are currently of intense research mainly due to the significant impact on biocompatibility and improvement of osseointegration of dental implants.

In the theoretical part are described types of titanium material and different methods of its surface modification. *In vitro* and *in vivo* biocompatibility and osseointegration tests are described as well.

The experimental work consists of two parts of experiments. In the first experiment, we examined how grain size of nanostructured titanium material influences the behaviour of fibroblastic as well as osteoblastic cells growth on its surface. The experimentally obtained data were statistically analysed and discussed. Grain size was proven to be an important factor that influenced not only the strength of material but also its interactions with cells.

The second experiment describes current methods used in the experimental evaluation of osseointegration of dental implants. The results of histological staining methods are illustrated and compared. A standardized and reproducible technique for stereological quantification of bone-implant contact is proposed and demonstrated. Surface modifications were verified to play a very important role in biocompatibility and osseointegration. Surface roughness significantly increases the contact area between implant and peri-implant bone. Practical recommendations for the experiment, harvesting of samples, tissue processing and quantitative histological evaluation are provided.

Key words: biocompatibility, osseointegration, titanium, nanotopography, dental implants, implant surface modifications, bone-implant contact

Abstrakt

Tato disertační práce se zabývá hodnocením biokompatibility a oseointegrace materiálů z nanostrukturovaného titanu používaných jako dentální implantáty. Titanové dentální implantáty a jejich povrchové úpravy jsou v současnosti intenzivně studovány pro jejich pozitivní vliv na biokompatibilitu a oseointegraci.

V teoretické části práce jsou popsány různé typy titanových materiálů a různé druhy povrchových úprav. Rovněž jsou popsány *in vitro* a *in vivo* metody testování biokompatibility a oseointegrace.

Experimentální část práce tvoří dvě skupiny experimentů. V první části je zjišťován vliv velikosti zrn na povrchu nanostrukturovaného titanu na chování a růst buněčných kultur fibroblastů a osteoblastů. Získaná experimentální data jsou statisticky analyzována a diskutována. Velikost zrn se jeví jako důležitý faktor, který ovlivňuje nejen pevnost materiálu, ale také interakci s buňkami.

Druhá část experimentu se zabývá metodami hodnocení oseointegrace dentálních implantátů. Jsou zde uvedeny a srovnány výsledky metod histologického barvení a je navržena reprodukovatelná metoda stereologické kvantifikace kontaktu kost-implantát. Bylo potvrzeno, že povrchové modifikace hrají velmi důležitou roli v biokompatibilitě a oseointegraci. Drsnost povrchu významně zvyšuje kontaktní plochu mezi implantátem a přiléhající kostí. V závěru jsou navržena doporučení pro správný sběr vzorků, jejich zpracování a kvantitativní histologické hodnocení.

Klíčová slova: biokompatibilita, oseointegrace, titan, nanotopografie, dentální implantáty, modifikace povrchu implantátu, kontakt kost-implantát

Table of Contents

List of Abbreviations

ASTM	American society for testing and materials
ATCC	American type culture collection
BC	Bone contact
BIC	Bone implant contact
BMP	Bone morphogenetic protein
CaP	Calcium phosphate
CCL153	Cellosaurus cell line of human foetal lung fibroblasts
CMFDA	5-chloromethylfluorescein diacetate
cpTi	Commercially pure titanium
DMSO	Dimethyl sulfoxide
ECAP	Equal channel angular pressing
ECM	Extracellular matrix
EDTA	Ethylenediaminetetraacetic acid
FAK	Focal adhesion kinase
FBS	Foetal bovine serum
FGF	Fibroblast growth factor
HA	Hydroxyapatite
HBD	Human beta defensin
HF	Hydrofluoric acid
HFL1	Human foetal lung fibroblasts
hFOB	Human foetal osteoblast cell line
HMG-CoA	5-hydroxy-3-methylglutaryl-coenzyme A
HTC	High throughput screening
hVIN-1	Anti-human vinculin antibody
ICC	Immunocytochemistry
IFN-γ	Interferon gamma
IL	Interface length
ILK	Integrin-linked kinase
MTT	3-(4,5-dimethylthiazol-2-yl)-2,5-diphenyltetrazolium bromide
NAD^+	Nicotinamide adenine dinucleotide
NADH	Nicotinamide adenine dinucleotide (reduced form)

nHA	Nanoscale hydroxyapatite
nTi	Nanostructured titanium
PDGF	Platelet-derived growth factor
RGD	Arginylglycylaspartic acid; tripeptide composed of L-arginine, glycine, and L-aspartic acid
SDS	Sodium dodecyl sulfate (*synonymously* sodium lauryl sulfate, SLS)
SEM	Scanning electron microscope
SLA	Sandblast, large-grit, and acid etching
SPD	Severe plastic deformation
Src	Sarcoma proto-oncogene, non-receptor tyrosine kinase
TGF-β	Transforming growth factor beta
TNF-α	Tumour necrosis factor alpha
TRITC	Tetramethylrhodamine
VEGF	Vascular endothelial growth factor
% v/v	Volume per volume
% w/v	Weight per volume

1 Introduction

The biocompatibility of synthetic substances (biomaterials) used for the replacement of biological tissues have always been a high-priority concern within the health care disciplines, including dentistry.

The history of the evolution of dental implants is an amazing journey through time. Since the beginning of mankind, humans have used dental implants of various kinds to replace missing teeth. In 2,500 BC, the Egyptians stabilized teeth with the gold wire ligature, about 500 BC, the Etruscans restored oral function with soldered gold bands and oxen bones, around 300 AD, the Phoenicians used teeth carved out of ivory and stabilized by gold wire in fixed bridge. Until the beginning of the 19th century innumerable substances were used as implants.[1] However, the real development of modern dental implantology began in 1952 with first experiments of Professor Per-Ingvar Brånemark. He developed a screw-shaped cylindrical implant designed from pure titanium. After implantation, he observed bone growing in such close proximity to the titanium implant that effectively adhered to the metal. Based on these observations, he and his colleagues later defined the concept of osseointegration as a direct and stable anchorage of an implant through the formation of bony tissue without the growth of fibrous tissue at the bone-implant interface.[2]

For osseointegration of dental implants, the suitable surface modifications, shape and materials are critical.[3] To be considered successful, an osseointegrated dental implant has to meet certain criteria in terms of function, tissue physiology, and user satisfaction.[4]

1.1 Classification of Implantable Materials in Dentistry

Materials used for the fabrication of dental implants can be divided in two different ways depending on their chemical or biological characteristics.

From a basic chemical point of view, dental implants can be categorised into one of the following three groups:

1) metals,
2) ceramics, and
3) polymers.

In addition, biomaterials can be classified based on the type of biologic response they elicit when implanted and the long-term interaction that develops with the host tissue. Three major types of biodynamic activity have been reported:

1) biotolerant,
2) bioinert, and
3) bioactive.[5,6]

Biotolerant materials are those that are not necessarily rejected when implanted into living tissue, but are surrounded by a fibrous layer in the form of a capsule.
Bioinert materials allow close apposition of bone on their surface, leading to contact osteogenesis.
Bioactive materials also allow the formation of new bone onto their surface, but ion exchange with host tissue leads to the formation of a chemical bond along the interface (bonding osteogenesis).
Bioinert and bioactive materials are also called osteoconductive, meaning that they can act as scaffolds allowing bone growth on their surfaces. They are a prerequisite for osseointegration.[7,8]

Biodynamic activity	**Chemical composition**		
	Metals	**Ceramics**	**Polymers**
Biotolerant	Gold		Polyethylene
	Cobalt-chromium alloys		Polyamide
	Stainless steel		Polymethylmethacrylate
	Zirconium		Polytetrafluoroethylene
	Niobium		Polyurethane
	Tantalum		
Bioinert	Commercially pure titanium	Aluminium oxide	
	Titanium alloy (Ti-6Al-4V)	Zirconium oxide	
Bioactive		Hydroxyapatite	

		Tricalcium phosphate	
		Tetracalcium phosphate	
		Calcium pyrophosphate	
		Fluorapatite	
		Brushite	
		Carbon: vitreous, pyrolytic	
		Carbon-silicon	
		Bioglass	

Table 1: Classification of dental implant materials.[7]

1.2 Titanium and Its Alloys

Since 1970, a number of new implant materials and designs have been developed, including the use of polymers, porcelain, high-density aluminium oxide (Alumina), bioactive glass (Bioglass) and carbon materials. Although nowadays, the most frequently used implant material is titanium which has become the gold standard in implant dentistry.

Titanium and its alloys are used in dentistry as prosthetic appliances thank to their unique combination of chemical, physical and biological properties. The American Society for Testing and Materials (ASTM International) recognizes different grades of commercially pure titanium (cpTi), and titanium alloys (Ti-6Al-4V, Ti-5Al-1.5B, Ti-6Al-7Nb, etc.). Clinically two forms of titanium have received the most interest - commercially pure titanium and Ti-6Al-4V.[9]

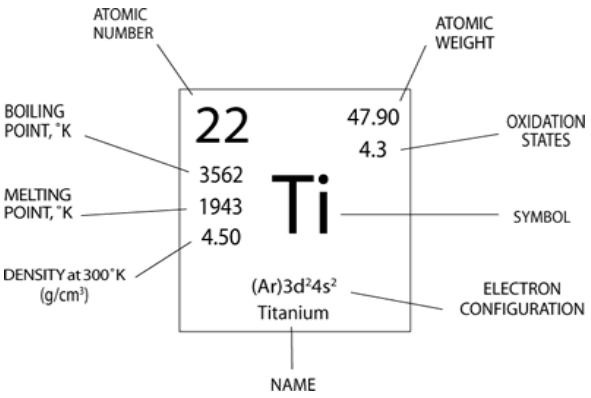

Figure 1: Chemical properties of pure titanium according to the periodic table.

1.2.1 Commercially Pure Titanium

Commercially pure titanium can be found in four different grades (see Table 2), which vary mainly in the content of oxygen.

ASTM Grade 1: In comparison to other grades, ASTM Grade 1 is chemically the purest one which makes the allergenic risk extremely low. It has the lowest mechanical strength among all grades but, at the same time, the highest formability. Alike the other grades, its corrosion resistance is excellent which is crucial for biocompatibility.

ASTM Grade 2: Grade 2 of titanium has very similar general properties like Grade 1. The main difference is in better mechanical resistance due to the higher content of interstitial elements iron and oxygen.

ASTM Grade 3: Grade 3 has the same ratio of iron; however, it has a higher content of nitrogen and oxygen. Mechanical properties are better in comparison to the Grade 2.

ASTM Grade 4: Grade 4 contains the most interstitial elements among all the grades – the content of iron is up to 0.5 % and content of oxygen up to 0.4 %. Mechanical properties as well as corrosion resistance are outstanding.

ASTM Grade	Ti [%]	Fe_{max} [%]	O_{max} [%]	H_{max} [%]	C_{max} [%]	N_{max} [%]
Grade 1	99,5	0,20	0,18	0,015	0,08	0,03
Grade 2	99,2	0,30	0,25	0,015	0,08	0,03
Grade 3	99,1	0,30	0,35	0,015	0,08	0,05
Grade 4	99,0	0,50	0,40	0,015	0,08	0,05

Table 2: Grades of cpTi.

1.2.2 Titanium Alloys

Titanium can be mixed with other chemical element(s) in order to improve its properties, such as strength, high temperature performance, creep resistance, response to ageing, heat treatments and formability.

The most commonly used alloys for dental implants contain 6% aluminium and 4% vanadium (Ti-6Al-4V). Aluminium serves to increase the strength and decrease the alloy weight. Vanadium decreases the alloys susceptibility to corrosion.[10,11]

Among other commonly elements used for titanium alloys belong, palladium, copper, zirconium, niobium, boron, molybdenum, tin and others. Potentially allergenic metal additives represent a significant disadvantage in comparison to cpTi.

1.2.3 Nanostructured Titanium

An important direction intensively developed in recent years is the investigation of mechanical properties of nanostructured materials. Nanomaterials are generally materials with grain size of 10^{-9} m. The formation of nanostructures in metals leads to higher strength but the costs remain very high (about 10 times more in comparison to cpTi). There is great interest in the processing of bulk, fully dense nanostructured metals and alloys. The fabrication of such materials based on severe plastic deformation (SPD) methods seems very interesting and useful. The first developments and investigation of nanostructured materials processed using SPD methods were carried out by Valiev et al. more than three decades ago.[12-14]

A promising and efficient method for the production of bulk ultrafine grained or nanostructured material is equal channel angular pressing (ECAP). The ECAP method involves the deformation of massive billets via pure shear followed by another possible deformation. The method was further developed and applied as an SPD method for processing structures with submicron and nanometric grain sizes. Nanostructured titanium produced in this way has both excellent biocompatibility and extraordinary mechanical properties.[15,16]

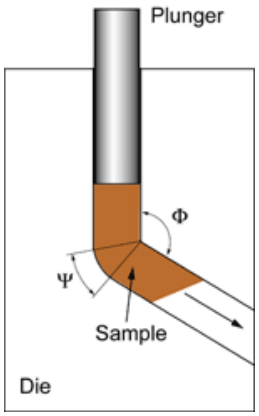

Figure 2: Principle of ECAP method[17]

It is known that nanostructuring of material changes its biological properties compared with material of the same chemical composition, but the mechanism of this phenomenon

has not yet been clarified.[18] The first evidence of such an effect was provided by Webster et al. in 1999, who found that osteoblast adhesion and bone formation significantly increased on nanostructured titanium surface compared with conventional titanium.[19] Since that time many *in vitro* as well as *in vivo* studies have investigated the impact of the nanostructured surface on the behaviour of cells and provide evidence that key biological processes, such as proliferation, gene expression, and initial protein adsorption that control such events, can be easily manipulated by modifying the nanotopography of implants.[20-23] It has also been proven that cells sense and react to nanotopography, by exhibiting changes in cell morphology, orientation, and cytoskeletal organisation.[24, 25]

1.3 Implant Surface Modifications

Surface treatments are normally carried out to modify yet maintain desirable properties of the substrate materials. The surface area can be increased remarkably by using proper modification techniques, either by addition or subtraction procedures. A surface treatment can also be classified into mechanical, chemical, and physical methods. In dental implant, the surface treatment is used to modify the surface topography and energy in order to improve wettability, increase cell proliferation and growth, and accelerate osseointegration process.

The interfacial interactions between recipient tissues and implanted material are limited to the surface layer of the implant and a few nanometres into the living tissues. Hence, the quality of dental implant depends on the properties of the surface.[26]

For example, osteoblasts have higher probability to adhere to a rough titanium surface while fibroblasts and epithelial cells adhere mainly to very smooth surfaces.[27,28] However, it has been shown that roughness may play an important role in the percentage of bone apposition as well as in the velocity of apposition. Roughness or acid conditioning of the surfaces can therefore significantly improve shear strength.

Besides optimizing the procedure, these surface characteristics may allow an earlier loading of the implant and extend the indications for implants in low-density alveolar bone and in regenerated bone.

1.3.1 Laser Treatment

The laser beam radiates electromagnetic energy that interacts with the titanium, taking it from a solid state to a plasma state. The extremely concentrated energy pulses of the laser allow micro-fabrication of the implant surface without any dangerous effects, such as thermal changes of material properties that can induce micro-fractures or alteration of the metal structure. This controlled micro-ablation is obtained using a low power setting. An important goal of laser treatment of an implant surface is to produce a surface with thousands of hemispheric pores for bone apposition.[29,30]

Nd:YAG laser is the most commonly used laser in the processing of titanium dental implants.[31]

1.3.2 Acid Etching

In acid etching, the use of acids on metal surfaces is not only to clean the surface but also to modify the roughness. A strong acid like hydrofluoric (HF), nitric (HNO_3), and sulphuric (H_2SO_4) or a combination of these acids is commonly used in this technique. Acid etched surfaces increase cell adhesion and bone formation, thus enhancing the osseointegration.[32]

Acid etching of titanium is of particular interest because it creates a micro-textured surface (a fine rough surface with micro pits of 1-3 μm and larger pits of approximately 6-10 μm) that appears to enhance early endosseous integration and the stability of the implant.[33] This may be related to the changes in surface roughness and chemical composition.

1.3.3 Plasma Spray Coating

A coating produces a rough implant surface that significantly improves the implant anchorage in the bone. Plasma coating works by blowing an inert gas through an intense electric arc. Down the arc, the coating material is introduced in the form of an extremely hot gas. The inert gas is broken into ions and electrons; this state is known as plasma. The titanium hydride (coating material) decomposes in the gas stream and forms droplets of molten metal that are projected onto the implant surface to build up a coating. The layer is typically 20-30 μm thick with a roughness of approximately 15 μm. Gases in titanium harden the metal, which is an advantageous enhancement for

the surface of an implant.[34] The bond strength between the porous plasma layer and the substrate is limited, but excessive treatment, such as exposure to an ultrasound source, is needed to cause this bond to fail. Titanium implants with this type of coating have an average BIC in cancellous bone of nearly 40 %, which is significantly higher than for smoothly polished or finely structured titanium implants, which have values of slightly over 20 %.[35]

1.3.4 Sand Blasting

Sand blasting roughens the surface of the implant and achieves both micro-retentive topography and increased surface area.[36,37] A sand-blasting treatment consists of the mechanical abrasion of surfaces using particles shot against the implant. The treatment produces a surface with a roughness that depends on the size, shape and kinetic energy of the particles. However, this increased roughness may reduce the endurance properties of metals.[38] Studies by Wennerberg et al.[39,40] demonstrated an optimal blasting particles of 75 μm, which made implant more resistant to torque and gave it greater bone-to-metal contact than did small (25 μm) or coarse (250 μm) particles. The optimal surface had an average height deviation of approximately 1.5 μm, resulting in a surface enlargement of 50 %. An average BIC around titanium sand-blasted implants is comparable to that observed around plasma-sprayed surfaces.

1.3.5 Sandblast, Large-Grit, and Acid Etching (SLA)

SLA is used to induce surface erosion by applying a strong acid onto the blasted surface. This treatment combines blasting with large-grit sand particles and acid etching sequentially to obtain macroroughness and micropits to increase the surface roughness as well as osseointegration.

Kim et al. observed that human osteoblasts grow well on the SLA surface which provides space for cell adhesion and proliferation. SLA surface possessed wide cavities (from 5 μm to 20 μm in diameter) and micropits (from ~0.5 μm to 3 μm in diameter), indicating an increase in the surface roughness and the surface area.[34]

1.3.6 Anodic Oxidation

In anodic oxidation, the implant is exposed to an electric arc with the implant serving as an anode. The implant surface is electrochemically modified to increase the thickness of the TiO_2 layer from 17-200 nm in conventional titanium implants to 600-1,000 nm. Thus, a porous surface microstructure with pore sizes of about 1.3-2.0 mm^2, a porosity of roughly 20 %, and a moderate degree of surface roughness of S_a = 1 µm is generated. Accordingly, this type of implant surface has also been referred to as titanium porous oxide or anodized titanium surface implant.

Nanostructured titanium surfaces generated by anodic oxidation have been shown to propagate adhesion, proliferation, and extracellular matrix deposition of human gingival fibroblasts.[42]

SURFACE TREATMENT	IMPLANT SYSTEM / SURFACE
Acid-etched Etching with strong acids increases the surface roughness and the surface area of titanium implants.	BIOMET 3i OSSEOTITE and NanoTite
Anodized This electrochemical process thickens and roughens the titanium oxide layer on the surface of implants.	Nobel Biocare TiUnite
Blasted Particles are projected through a nozzle at a high velocity onto the implant. Various materials, such as titanium dioxide, aluminium dioxide and hydroxyapatite (HA) are often used.	DENTSPLY Implants ASTRA TECH TiOblast, Zimmer Dental MTX, Inclusive Tapered Implants
Blasted and acid-washed / etched Implants undergo a blasting process. Afterward, the surface is either washed with non-etching acid or etched with strong acids.	CAMLOG Promote, DENTSPLY Implants FRIALIT and FRIADENT plus, Straumann SLA
Hydroxyapatite (HA) HA is an osteoconductive material that has the ability to form a strong bond between the bone and implant.	Implant Direct (various), Zimmer Dental MP-1
Laser ablation High-intensity pulses of a laser beam strike a protective layer that coats the metallic surface. As a result, implants demonstrate a honeycomb pattern with small pores.	BioHorizons Laser-Lok

Plasma-sprayed Powdery forms of titanium are injected into a plasma torch at elevated temperatures.	Straumann ITI titanium plasma-sprayed (TPS)

Table 3: Overview of implants and their respective surface treatments.[43]

1.3.7 Hydrophilic Implant Surface

An important modification is the improvement of the wettability of implant surfaces due to the biological implications of hydrophilicity, from the initial contact between an implant surface and host interface, which involves interactions with water and ions via conditioning by the formation of protein-rich films, up to the level of cellular interactions. The general idea is that when wettability is increased, biocompatibility is enhanced, promoting interactions between an implant surface and the biological environment, allowing for the activation of cellular activity most likely modulated by the energy of implant surface.

Conventional surfaces are kept dry and exposed to air, making them hydrophobic due to the adsorption of carbon and the hydrocarbons present in the air and reducing the wetting of the implant by the surrounding biological environment; this process makes it difficult for proteins to be adsorbed and for cellular responses to be induced. One of the principal strategies for preventing a decrease in the surface energy of titanium implants is the liquid isolation of the surface of TiO_2 not contaminated by the atmosphere. Compared to conventional surfaces, these modified surfaces favour the adsorption of proteins and are able to promote the activation of osteoblasts toward a more osteogenic phenotype. These phenomena suggest that the increased bone formation observed on the modified surface of these implants should be due to the stimulating effect of high surface energy on osteoblasts. Previous studies have shown that a hydrophilic surface is beneficial for gene expression, osteoblast behaviour, bone mineralization and early osseointegration.[44]

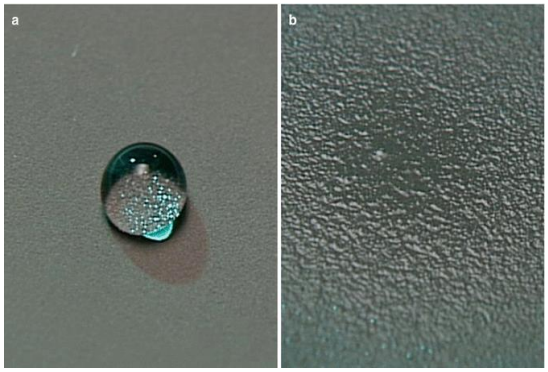

Figure 3: Drop of water on hydrophobic SLA surface (a) and on hydrophilic modSLA surface (b). Increased hydrophilicity on modSLA surface indicated by complete dispersion of water drop (b, no measurable contact angle between water drop and surface); however, no dispersion of water drop on hydrophobic SLA surface (a, obvious measurable contact angle between water drop and surface).[45]

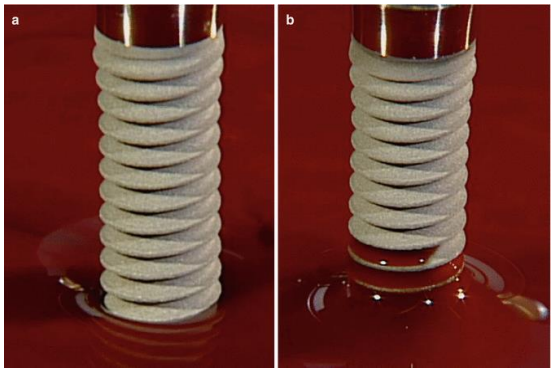

Figure 4: The increased surface hydrophilicity can also induce an accelerated covering of the implant surface with blood from the peri-implant soft and bone tissue during placement of the implant, compared to hydrophobic SLA surfaces, thus accelerating the initial implant healing period.[45]

1.3.8 Titanium Materials Coating

Bioactive surface coatings of titanium dental implants help to optimise implant stability by interacting with natural cascades of osseointegration, to improve peri-implant soft tissue integration, and to reduce peri-implantitis by impairing bacterial adhesion to the implant surface. Coatings which are used in dental implantology researches nowadays are briefly explained below.

1.3.8.1 Hydroxyapatite and Nanocomposite Coating

Hydroxyapatite (HA) is a very stable biological form of CaP that strengthens the organic matrix by mineralization. Biomimetic surface techniques attempt to promote osseointegration by integration of a singular component or a combination of these elements into the implant surface.

HA coatings resemble a reservoir of calcium and phosphate[46] in addition to their biomimetic property. For several years, titanium plasma spraying was the commonly applied technique to deposit CaP on implant surfaces.[47] A powder was dispersed into a plasma torch that is targeted on the implant resulting in a CaP thickness of 40-50 μm.[48] Uncertainty exists regarding the long-term stability of plasma-sprayed HA coatings[49] and long-term clinical outcomes were poor.[50]

A recently introduced surface treatment generates a hydrophilic monolayer of multiphosphonic acid molecules on the outside of the implant surface, thus imitating natural hydroxyapatite (SurfLink, Nano Bridging Molecules, Gland, Switzerland).[51]

To simulate the biological environment of nanoscale crystals in native bone tissue, nanotechnology has become of essential importance to compose nanoscale hydroxyapatite (nHA) containing implant surfaces.[52]

Extensive work has been carried out to transfer nanotechnology to HA coatings. nHA is used as a single compound coating or as part of a composite in combination with carbon nanotubes, collagen, titanium dioxide, bioglass, silica, or ceramic oxide. A major advantage of nanocomposites is the ability to adjust the mechanical characteristics of the implant to those of natural bone, for example, to avoid negative stress shielding.[42]

1.3.8.2 Growth Factors

In haemostasis primary phase of osseointegration, platelets, which have been liberated to the alveolar bone from damaged vessels, degranulate and release specific growth factors that initiate the second phase of osseointegration, the inflammatory phase. These factors embrace fibroblast growth factor (FGF), platelet-derived growth factor (PDGF), and transforming growth factor beta (TGF-β). Macrophages resemble a second important source of growth factors. Upon elimination of cell detritus, these cells release VEGF (vascular endothelial growth factor), PDGF, and FGF to initiate the proliferative

phase of osseointegration. VEGF induces neoangiogenesis that is pivotal for osteogenesis.[53]

Bone morphogenetic proteins (BMPs) were first described in 1965 and contain a group of at least 18 growth factors that belong to the TGF-β family.[54] *In vivo*, BMPs are released from osteoblasts, platelets, and endothelial cells and are deposited into the bone matrix until being liberated during socket preparation. BMPs regulate genes for collagen, alkaline phosphatase, and osteopontin. BMP2, BMP4, and BMP7 exclusively stimulate bone formation. To acquire an adequate yield of BMPs, these proteins have to be produced in a recombinant technique.[55]

1.3.8.3 Extracellular Matrix Proteins

In the proliferative phase of osseointegration, fibroblasts are triggered by FGF to secrete extracellular matrix proteins like collagen, chondroitin sulfate, fibronectin, vitronectin, and other proteoglycans. The extracellular matrix provides crucial guidance for osteoprogenitor cells that migrate to the implant via interaction of integrins on the cell surface and RGD motifs of fibronectin. Osteoblasts have been proposed to originate from subset of mesenchymal stem cells that line minor vessels and are known as pericytes. Upon the release of BMP, these cells differentiate into osteoblasts.[53]

Dental implants coated with extracellular matrix proteins have shown a positive effect on peri-implant bone formation in preclinical studies.[56]

1.3.8.4 Peptides

Peptides are biomolecules composed of short sequences of amino acids. They resemble fragments of larger proteins. Particular peptides that facilitate cell adhesion in osseointegration or that exert antibacterial effects have been employed to design new implant surfaces.

The RGD peptide, a tripeptide composed of L-arginine, glycine, and L-aspartic acid, is an important sequence of extracellular matrix proteins that acts as a binding site for integrin receptors in adhesion and migration of osteogenic cells. Broggini et al.[57] reported no significant effect of RGD peptide coatings in a minipig model compared to SLActive control implants.

Human beta defensins (HBDs) are peptides that convey antibacterial effects on epithelial borders. In cell experiments, HBDs exhibited biocompatibility and were able to promote proliferation of osteoblasts and mesenchymal stem cells.[41]

1.3.8.5 Messenger Molecules

The remodelling phase succeeds the proliferative phase. Woven bone is transformed into load oriented trabecular bone.[53]

In bone remodelling, osteoblasts interact closely with osteoclasts. Sclerostin is one of the messenger molecules that mediate the osteoblast-osteoclast interaction. It is secreted by osteocytes and serves as an inhibitor of osteogenesis by blocking osteoblastic bone formation.[58]

1.3.8.6 Drug Coatings

HA coatings have been successfully used as local drug delivery systems.

Statins inhibit the HMG-CoA reductase and are prescribed in dyslipidaemia. When incorporated in the implant surface, statins have been claimed to trigger the local liberation of BMPs, thus promoting osseointegration.

Bisphosphonates are antiresorptive drugs that influence bone metabolism mainly by inhibition of osteoclasts. Common indications include metastatic bone disease or osteoporosis. Peter et al.[59] demonstrated in a rat model that implants with a Zolendronate containing HA coating yield a higher peri-implant bone density and promote increased mechanical fixation. In an osteoporotic rat model, Stadlinger et al.[60] demonstrated increased BIC and a higher level of bone mineralization of Zolendronate loaded implants.

Tetracycline-HCl functions as an antimicrobial agent capable of killing microorganisms that may be present on the contaminated implant surface. It also effectively removes the smear layer as well as endotoxins from the implant surface. Further, it inhibits collagenase activity, increases cell proliferation as well as attachment and bone healing. Tetracycline also enhances blood clot attachment and retention on the implant surface during the initial phase of the healing process and thus promotes osseointegration.[42]

Implant coating	Example	Studies	Outcome
Carbon coating	Currently not on the market; still not being investigated	*In vitro*, *in vivo*, and clinical studies	Improved biologic properties and histocompatibility but studies are still under way
Bisphosphonates	Currently not on the market; still not being investigated	No long-term studies available	No long-term studies available
Bone stimulating factors	Currently not on the market; still not being investigated	Pilot animal studies and clinical studies	Studies are still under way
Bioactive glasses and ceramics	Currently not on the market; still not being investigated	Chemical, *in vivo*, and *in vitro* studies	Studies are still under way
Fluoride coating	OsseoSpeed	*In vitro* studies	Selective osteoblast differentiation results
Hydroxyapatite (HA)	Restore Implant system	*In vitro*, *in vivo*, and retrieval studies	Most commonly used type of implant coating; other implant coating studies mainly use HA as a control
Titanium/titanium nitride	IonFusion	*In vitro*, *in vivo*, and clinical studies	Titanium mechanical properties are considered in relation to the degree of osseointegration

Table 4: Summary of implant coatings.[61]

1.4 Biocompatibility and Its Measuring

Biocompatibility is formally defined as the ability of a material to elicit an appropriate biological response in a given application in the body. Inherent in this definition is the idea that a single material may not be biologically acceptable in all applications. Whether or not a material is biocompatible therefore depends on the physical function for which the material will be used and the biological response that will be required from it – e.g., an appropriate biological response for a dental implant is osseointegration.

Measuring the biocompatibility of a material is not simple, and the methods of measurement are evolving rapidly as more is known about the interactions between dental materials and oral tissues and as technologies for testing improve. Several varieties of tests are currently used to ensure that new materials are biologically acceptable. These tests are classified as *in vitro, in vivo* (animal) and usage tests.[62]

Test	Advantages	Disadvantages
***In vitro* tests**	Quick to perform	Relevance to in vivo is questionable
	Least expensive	
	Can be standardised	
	Large-scale screening	
	Good experimental control	
	Excellence for mechanism of interactions	
***In vivo* tests**	Allow complex systemic interactions	Relevance to use of material is questionable
	Response more comprehensive than *in vitro* tests	Expensive
	More relevant than *in vitro* tests	Time consuming
		Legal/ethical concerns
		Difficult to control
		Difficult to interpret and quantify
Usage tests	Relevance to use of material is assured	Very expensive
		Very time consuming
		Major legal/ethical concerns
		Can be difficult to control
		Difficult to interpret and quantify

Table 5: Advantages and disadvantages of biocompatibility tests.[62]

1.4.1 *In Vitro* Evaluation Methods

Biocompatibility *in vitro* tests require placement of a material or its component in contact with isolated biological system like a cell, enzyme, or other. They are executed out of the living organism. This contact can be either direct, when the material contacts

the cell system without barriers, or indirect, when there is a barrier of some sort between the material and the cell system. Material in the direct tests can be either physically present with the cells, or there can be only some extract from the material which contacts the cell system.

In vitro tests are used to measure cytotoxicity or cell growth, metabolic or other cell function or the effect on the genetic material in a cell (mutagenesis assays). Often there is overlap in what a test measures.

In vitro tests have many significant advantages compared to other types of biocompatibility tests – they are relatively quick, can be standardised, are suitable to large-scale screening, and generally cost less than animal tests.

The major disadvantage of *in vitro* tests is their questionable relevance to the final *in vivo* use of material. Another significant disadvantage includes the lack of inflammatory and other tissue-protective mechanisms in the *in vitro* environment. It should be pointed out that *in vitro* tests alone cannot entirely predict the overall biocompatibility of a material.[63]

1.4.1.1 Cells Used for *in Vitro* Assays

Standardization of *in vitro* tests is a primary concern. Two types of cells can be used for *in vitro* assays – primary cells and continuously grown cells (cell lines).

Primary cells are those cells taken directly from an animal and cultured. These cells will grow for only a limited time in culture but usually retain many of the characteristics of cells *in vivo*. For measuring cytotoxicity of materials, primary cell cultures seem to be more relevant than continuous cell lines. However, primary cells, being from a single individual, have limited genetic variability, may harbour viral or bacterial agents that alter their behaviour, and often rapidly lose their *in vivo* functionality once placed in culture.[63]

Continuously grown cells or cells lines are cells that have been transformed previously to allow them to grow more or less indefinitely in culture. Because of this transformation, these cells do not retain all *in vivo* characteristics, but they do consistently exhibit those features that they do retain. Genetic and metabolic stability of continuous cell lines contributes significantly toward standardizing assay methods.

Human foetal osteoblast cell line 1.19 (hFOB 1.19) provides a homogenous, rapidly proliferating model system for studying normal human osteoblast differentiation,

osteoblast physiology, and hormonal, growth factor, and other cytokine effects on osteoblast function and differentiation.[64] Immortalized human gingival fibroblasts (hTERT) play important role in testing the biocompatibility and toxicity of new dental materials.[65]

Finally, both primary and continuous cells play an important role in *in vitro* testing; and both should be used to assess materials.

1.4.1.2 Cell Adhesion to Implantable Material

After implantation, the fate of the implant surface has been described as a "race for the surface" among protein adsorption, host cell adhesion, and bacterial adhesion.[66]

The first step a cell has to take to be able to differentiate and express its potential is often adhesion on a substrate, whatever this one might be. This adhesion or attachment of the cell occurs through specific structures, such as hemidesmosomes and focal adhesions. Specific protein structures (receptors) such as integrins in focal adhesions and cadherins in hemidesmosomes allow this attachment.[67]

Different treatments for different biomaterials have been proposed to enhance the properties of the surface of these biomaterials to promote cellular adhesion.

Cell–matrix adhesions are discretely distributed on the cell surface and mediate cell interactions with the ECM. They are essential for cellular functions, such as cell rolling, migration, differentiation, tissue remodelling and homeostasis. Mechanical force plays a key role in adhesion maturation.

Throughout the maturation of cell-matrix adhesions, integrins are key players. Integrins are a family of transmembrane proteins: the ectodomain of integrin binds to its ECM ligands and the cytoplasmic tail links to the cytoskeleton via adaptor molecules including talin, actin, vinculin, and tensin, thereby connecting the intracellular cytoskeletons to the ECM through the adhesion sites and transmitting bidirectional signals. Integrins are the most intensively studied and best characterized among cell-matrix adhesion proteins.[68]

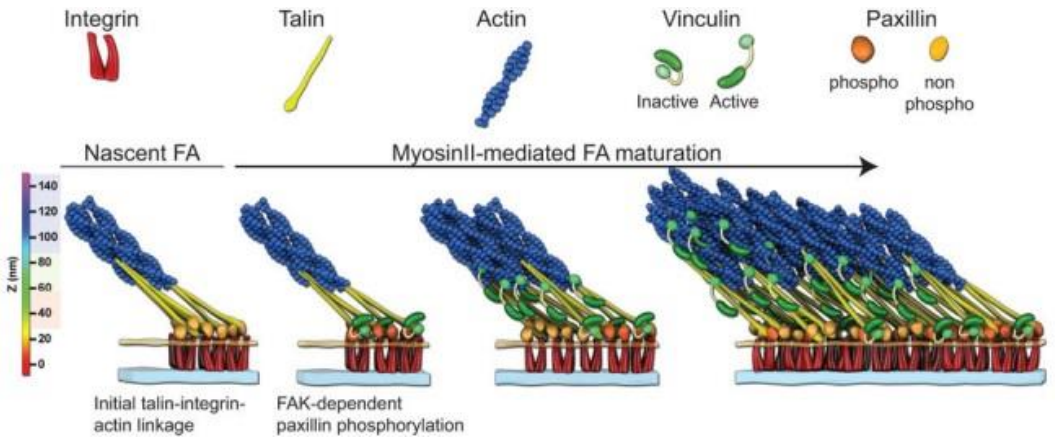

Figure 5: Interconnection of intra- and extracellular proteins.[69]

1.4.1.3 Immunocytochemistry

Immunocytochemistry (ICC) is a common laboratory technique where a specific primary antibody is used to bind on a specific protein or antigen in cells in order to visualize the localization of such a protein or antigen. The primary antibody allows visualization under fluorescence microscope when it is bound by a secondary antibody which has a conjugated fluorophore. ICC allows for the evaluation whether or not cells in a particular sample express the antigen. In cases where an immunopositive signal is found, ICC is also able to determine which sub-cellular compartments are expressing the antigen.

1.4.1.4 Cell Viability and Proliferation

Cell-based assays are often used to determine if the test molecules have effects on cell proliferation or show direct cytotoxic effects that eventually lead to cell death. These assays are also helpful for measuring receptor binding and a variety of signal transduction events that may involve the expression of genetic reporters, monitoring organelle function, or trafficking of cellular components. Indifferent to the type of cell-based assay being used, it is substantial to know the amount of viable cells which remained at the end of the experiment.[70]

The MTT (3-[4,5-dimethylthiazol-2-yl]-2,5 diphenyl tetrazolium bromide) assay is based on the conversion of MTT into formazan crystals by living cells, which determines mitochondrial activity. Since for most cell populations the total mitochondrial activity is related to the number of viable cells, this assay is widely

used to measure the in vitro cytotoxic effects of drugs on cell lines or primary patient cells.[71] The MTT assay was the first homogeneous cell viability assay developed for a 96-well format that was suitable for high throughput screening (HTS). The MTT assay technology has been widely adopted and remains popular in academic labs as evidenced by thousands of published articles. The MTT substrate is prepared in a physiologically balanced solution, added to cells in culture, usually at a final concentration of 0.2-0.5 mg/ml, and incubated for one to four hours. The quantity of formazan (presumably directly proportional to the number of viable cells) is measured by recording changes in absorbance at 570 nm using a plate reading spectrophotometer. A reference wavelength of 630 nm is sometimes used, but not necessary for most assay conditions.

Viable cells with active metabolism convert MTT into a purple coloured formazan product with an absorbance maximum near 570 nm. When cells die, they lose the ability to convert MTT into formazan, thus colour formation serves as a useful and convenient marker of only the viable cells. The exact cellular mechanism of MTT reduction into formazan is not well understood, but likely involves reaction with NADH or similar reducing molecules that transfer electrons to MTT.[70]

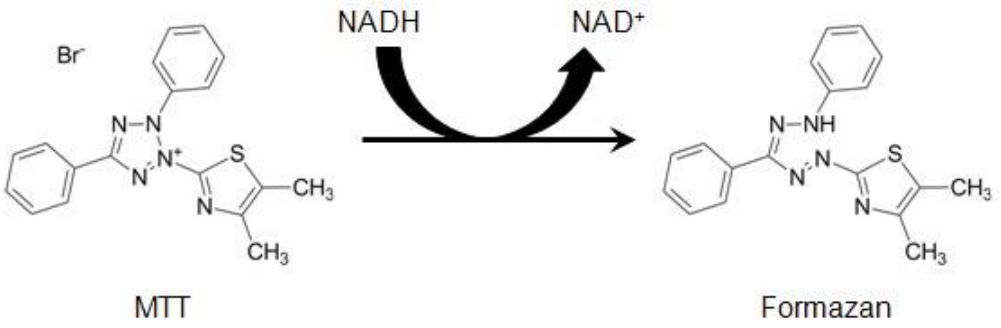

Figure 6: Transformation of MTT to formazan by living cells.[70]

The formazan product of the MTT tetrazolium accumulates as an insoluble precipitate inside cells as well as being deposited near the cell surface and in the culture medium. The formazan must be solubilized prior to recording absorbance readings. A variety of methods have been used to solubilize the formazan product, stabilize the colour, avoid evaporation, and reduce interference by phenol red and other culture medium components. Various solubilisation methods include using: acidified isopropanol,

DMSO, dimethylformamide, SDS, and combinations of detergent and organic solvent. Acidification of the solubilizing solution has the benefit of changing the colour of phenol red to yellow colour that may have less interference with absorbance readings. The pH of the solution can be adjusted to provide maximum absorbance if sensitivity is an issue.[70]

1.4.2 *In Vivo* Evaluation Method

Goal of *in vivo* evaluation methods is to determine biocompatibility or safety in a biological environment. The tests are carried out to determine that the device performs as intended and presents no significant harm to patient or user. *In vivo* evaluation involves implanting a sample of the material in test animals. The geometry of the test sample should simulate that of the implant device. Surface textures and relative size should be similar. If there is a possibility of wear debris in adjacent tissue, the particles of the material similar in size and shape to wear debris should be implanted with implant specimen. The implant specimen may be placed in muscle or cortical bone.

1.4.2.1 Osseointegration

Osseointegration is defined as a direct connection between living bone and a load-carrying endosseous implant at the light microscopic level[72] or as a time-dependent healing process whereby clinically asymptomatic rigid fixation of alloplastic materials is achieved, and maintained, in bone during functional loading.[73]

Direct bone healing, as it occurs in defects, primary fracture healing and in osseointegration, is activated by any lesion of the pre-existing bone matrix.

When the matrix is exposed to extracellular fluid, non-collagenous proteins and growth factors are set free and activate bone repair. Once activated, osseointegration follows a common, biologically determined program that is subdivided into three stages:

1) incorporation by woven bone formation;
2) adaptation of bone mass to load (lamellar and parallel-fibred bone deposition);
3) adaptation of bone structure to load (bone remodelling).[74]

Osseointegration requires primary stability, enabling bone progenitor cells from the existing bone or bone marrow to deposit new bone matrix around the implant material.

The implant integration into the bone tissue provides biomechanical stability and enables load-bearing.

1.4.2.2 Bone-Implant Contact (BIC)

Although the definition of osseointegration does not state the proportion of bone in contact with the implant surface, one of the most used variables in histomorphometric analysis of implants is the fraction of surface areas of mineralized bone in contact with the implant surface; so called bone-implant contact (BIC).

Histomorphometry is an established method to determine the extent of osseointegration and the rate of healing of dental implants; it can be used to measure the percentage of BIC.

Implant ground sections in situ are relatively thick sections (20-40 µm) and therefore only a few sections are obtainable from a bone-implant block. When serial sections of bone-implant specimens are cut thoroughly, a 'shadow effect' will appear at the peripheral section.[75]

Experimental trials on animal models revealed that implants with roughened surfaces had a better early anchorage in bone tissue and a higher percentage of BIC than implants with smooth surfaces.[76,77] Repeating the same experiments in human studies produced the same results.[78-81] The successful clinical use of micro-rough titanium implant surfaces have laid the foundations for developing further surface topographies to promote enhanced peri-implant bone apposition, during the early stages of bone regeneration.

2 Aim and Objectives

The aim of the first study was to measure cell adhesion and viability on the titanium and nanostructured titanium surfaces of dental implants and to evaluate if any of the six studied materials is better than others with respect to biocompatibility and cell proliferation.

Examined samples of titanium had grain sizes of 160 nm, 280 nm, and 2,400 nm. For each grain size there were two types of sample: cross-section (−) and longitudinal section (+).

Hypotheses:

1) grain size influences strength of material as well as its interactions with cells;
2) the smaller grains, the better biocompatibility (incl. wettability, cell adhesion and proliferation) and cell viability;
3) different sections differ in viability of cells grown on its surface – crystallographic texture is more important than grain sizes;
4) all tested materials are cytocompatible.

The fundamental aim of the second study was to review the experimental methods currently being used to evaluate the osseointegration of nanostructured titanium implants using animal models, to illustrate and compare the results of histological staining methods used in dental implantology and, finally, to develop and demonstrate a standardized and reproducible technique for stereological quantification of bone-implant contact. It was also expected to collect practical knowledge useful for further examinations.

In this study, dental implants with various surface modifications were used, as e.g., laser-treated, acid-etched, plasma-coated, and sand-blasted surface. Animal species and target bones were carefully compared in terms of the ratio of compact to spongy bone.

***Hypotheses*:**

1) surface modifications play a very important role in biocompatibility and osseointegration;
2) mechanically added surface roughness significantly increases the contact area between the implant surface and the peri-implant bone.

3 Experimental Work

3.1 Comparison of Fibroblast and Osteoblast Response to Cultivation on Titanium Implants with Different Grain Sizes

3.1.1 Titanium

All the samples were obtained from commercially pure titanium by the ECA pressing method from cpTi grade 2. They have a cylinder shape with a diameter of 4.98-5.05 mm and height of 2.93-3.01 mm (Figures 7a and 7b). Used samples of titanium have grain sizes of 160 nm, 280 nm, and 2,400 nm. For each grain size there were two types of sample: cross-section (−) and longitudinal section (+) (Figures 7c and 7d, resp.).

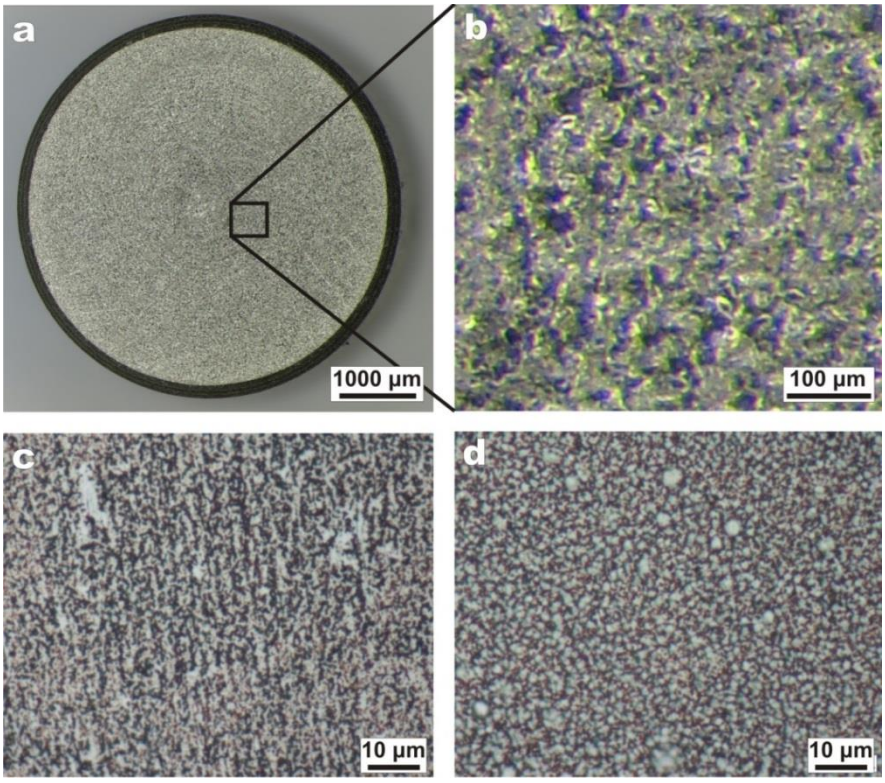

Figure 7: Photographs illustrating nanostructured titanium samples (a – macroscopic image; b – details of the surface; c – SEM images of longitudinal cross-section; d – SEM images of transversal cross-section).

Each implant was cleaned and sterilised before usage. The procedure contains incubation in a trypsin solution (0.25% (w/v) Trypsin-0,53 nM EDTA solution, PAA Laboratories GmbH, Austria) (30 minutes, 37 °C), followed by incubation in an ultrasonic bath (20 minutes, 25 °C), incubation in acetone (20 minutes, 25 °C), and at the end rinse in 70% ethanol and deionised water. Finally the implants were sterilised by autoclaving.

3.1.2 Surface Roughness Measuring Method

The surface roughness of each sample was measured three times using a mechanical contact profilometer Surtronic 25 (Taylor Hobson, UK). Surface roughness of samples was quantified by arithmetical mean roughness R*a* (defined as arithmetic average of the absolute values of the profile height deviations from the mean line) and ten-point mean roughness Rz (defined as the sum of the average value of absolute values of the heights of five highest profile peaks and the depths of five deepest profile valleys measured in the vertical magnification direction from the mean line). The surface roughness was measured at a traverse speed of 1 mm/s with a diamond-tipped stylus with 5 µm radius. The average of the three measurements was recorded as the mean surface roughness for each specimen.

3.1.3 Viability and Proliferation Measuring Method

Cell Cultures

Both used cell lines were obtained from ATCC (American type culture collection, Rockville, MD, USA) and cultured in accordance with ATCC recommendations. Culture media were refreshed as needed. Human foetal lung fibroblasts (HFL1, ATCC, and CCL153) were cultivated in F12K Medium (PAA Laboratories GmbH, Austria) supplemented with 10% (v/v) foetal bovine serum (FBS, PAA Laboratories GmbH, Austria), 100 U/mL penicillin and 100 mg/mL streptomycin (PAA Laboratories GmbH, Austria), and 2.5 mML-glutamine (Gibco, Life Technologies, Paisley, UK) at 37 °C under 5% CO_2 in a humidified incubator.

A human foetal osteoblast cell line, hFOB 1.19 (ATCC, CRL11372), established by Harris et al., was grown in a 1:1 mixture of Ham's F12 Medium and Dulbecco's Modified Eagle's Medium with 2.5 mML-glutamine (without phenol red)

(Gibco, Life Technologies, Paisley, UK) supplemented with 10% (v/v) FBS and 0.3 mg/mL geneticin (G418, Serva Electrophoresis GmbH, Heidelberg, Germany).
Cells were maintained at 34 °C under 5% CO_2 in a humidified incubator.

Cell Viability and Proliferation

Cell proliferation after 48 hours from plating was assessed by MTT viability and proliferation assay (ScienCellTMResearch Laboratories, Carlsbad, CA, USA) according to the manufacturer's instruction. This assay is based on the conversion of pale yellow tetrazolium MTT to purple formazan crystals, which can be solubilised and then spectrophotometrically quantified.

The samples of implants were placed into a 96-well plate (TPP, St. Louis, MO, USA). Cells harvested with trypsin solution from Petri dishes were resuspended in culture medium and seeded at a density of approximately 500,000 cells/mL onto the top of the discs of nanostructured titanium in 20 μL volume. As positive control, cells grown directly on the 96-well tissue culture plate were used.

After 48-hour incubation, cells were washed with phosphate-buffered saline (PBS) and incubated with 10 μL MTT (25 mg/mL) solution at 37 °C. After 4 hours, 100 μL of MTT solubilisation buffer (equal to the volume of original culture medium) was added to each well and the insoluble formazan formed was dissolved by pipetting up and down.

The absorbance was measured at 570 nm (spectrophotometer Nano Drop 1000, Thermo Fisher Scientific, Waltham, MA, USA), subtracting the background absorbance determined at 690 nm.

3.1.4 Fluorescence Microscopy

Cells Staining

Cultured cells were stained with CellTracker Green 5-chloromethylfluorescein diacetate (CMFDA) (Molecular Probes, Inc., Eugene, Oregon, USA) according to the manufacturer's instruction. Briefly, cells were properly washed with PBS and incubated with 4 μM CMFDA working solution for 30 minutes at 37 °C. Then, the dye working solution was replaced with fresh, prewarmed medium and the cells were incubated for another 30 minutes at 37 °C. Stained cells were analysed using an Olympus IX 70 fluorescent microscope equipped with Cell R system at 40x, 100x, and 400x magnification.

The initial cell attachment and the spreading of the cells on the substrate with different grain size were examined after 6 and 24 hours, respectively. The area occupied by the cells was assessed by analysis of gained images by the programme ImageJ (W. S. Rasband, U. S. National Institutes of Health, Bethesda, Maryland, USA).

Immunocytochemistry

The samples of implants were placed into a 24-well plate. Five hundred cells were seeded onto the top of the discs of nanostructured titanium cells and incubated for 2 or 48 hours. Fixation was performed by 3% formaldehyde in PBS for 15 minutes at 37 °C followed by three rinses with PBS. Permeabilisation was carried out by incubation with 0.1% triton X-100 solution in PBS for 10 minutes at room temperature. Blocking with 2% normal goat serum (Milipore, Billerica, MA, USA) followed for 1 hour at 4 °C. Each sample was double stained. Indirect immunofluorescence staining was done with a mouse monoclonal antivinculin antibody hVIN-1 diluted in PBS (1:100) and goat α-mouse Atto488 conjugated secondary antibody. For actin staining, Phaloidin-Tetramethylrhodamine B isothiocyanate (TRITC) was added into the solution of secondary antibody in PBS (0.75 Atto488 : 1.5 TRITC : 100 PBS) (all Sigma–Aldrich, St. Louis, MO, USA). Incubation with primary antibody was overnight. The second incubation was 2 hours at room temperature in the dark. Samples were analysed using an Olympus IX 70 fluorescent microscope equipped with a Cell R system at 40x, 100x, and 400x magnification.

3.1.5 Statistical Analysis

Microscopic analysis was carried out two times at a minimum, using two samples per group. In case of MTT assay, two independent experiments with quadruplicate measurements were performed. Cell viability was compared by analysis of variance (ANOVA). If ANOVA indicated a significant difference ($P < 0.05$) statistical comparisons were computed by two-tailed unpaired *t*-test with the value of significance $P < 0.05$. Statistical analysis was performed using the SigmaPlot 12.5 software (Systat Software Inc., San Jose, California, USA).

3.1.6 Results

3.1.6.1 Sample Characterization

Sample characterization was performed by SEM. Figure 8 shows SEM images of the titanium sample surfaces. The surface roughness quantified by arithmetical mean roughness *Ra* and ten-point mean roughness *Rz* of each sample is shown in Figure 9. Values of *Ra* were between 0.3 and 0.6 μm and *Rz* between 1.5 and 3.0 μm. We did not find any significant differences in surface roughness (for both parameters *Ra* and *Rz*) among studied materials ($P = 0.1097$ and $P = 0.0623$, resp.).

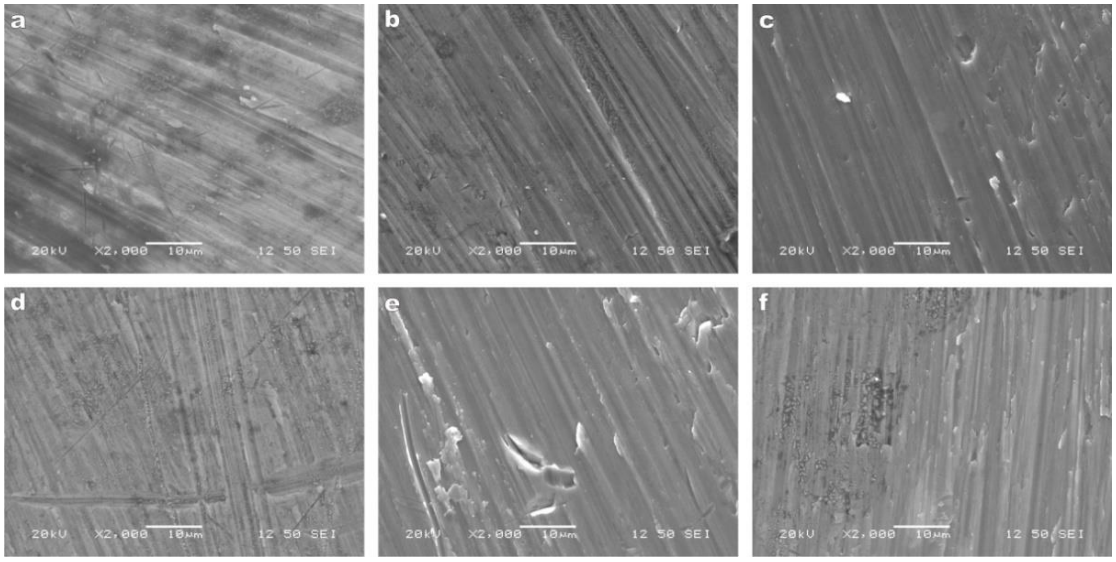

Figure 8: SEM photographs of the sample surfaces with different grain sizes and sections (a, b, c – SEM images of longitudinal cross-section with grain sizes of 160, 280, and 2,400 nm, respectively; d, e, f – SEM images of transversal cross-section with grain sizes of 160, 280, and 2,400 nm, respectively).

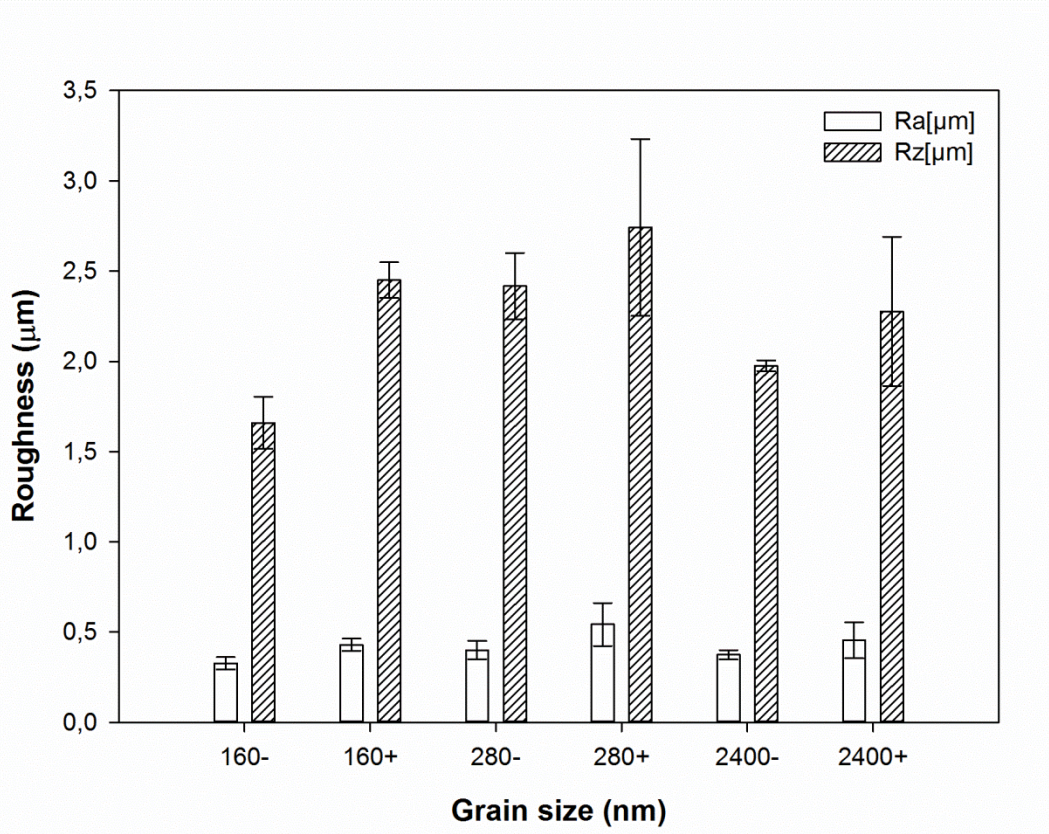

Figure 9: The surface roughness expressed by arithmetical mean roughness R*a* and ten-point mean roughness Rz. The standard errors were calculated from three independent measurements. Error bars indicate means ± standard deviations.

3.1.6.2 Cell Viability and Proliferation

Cell Adherence and Spreading

The initial cell attachment within the first 6 hours was significantly slower on titanium materials with grain size 2,400 (− and +) nm and 280 (− and +) nm, when compared with control (tissue culture plate) (P = 0.0043) (Figures 10, 11a, and 11c). On the surface with 160 (− and +) nm grains. The cells adhered as well as on control plate. The area occupied by fibroblasts on all studied materials reached very similar values as the control at 24 hours of cultivation (Figures 10, 11b, and 11d.

We also analysed differences between particular materials. The occupied area after 6 hours was significantly higher on material 160− in contrast to 280− and both types of 2,400 (− and +) (P < 0.0001; P = 0.0170; P = 0.0259; resp.).

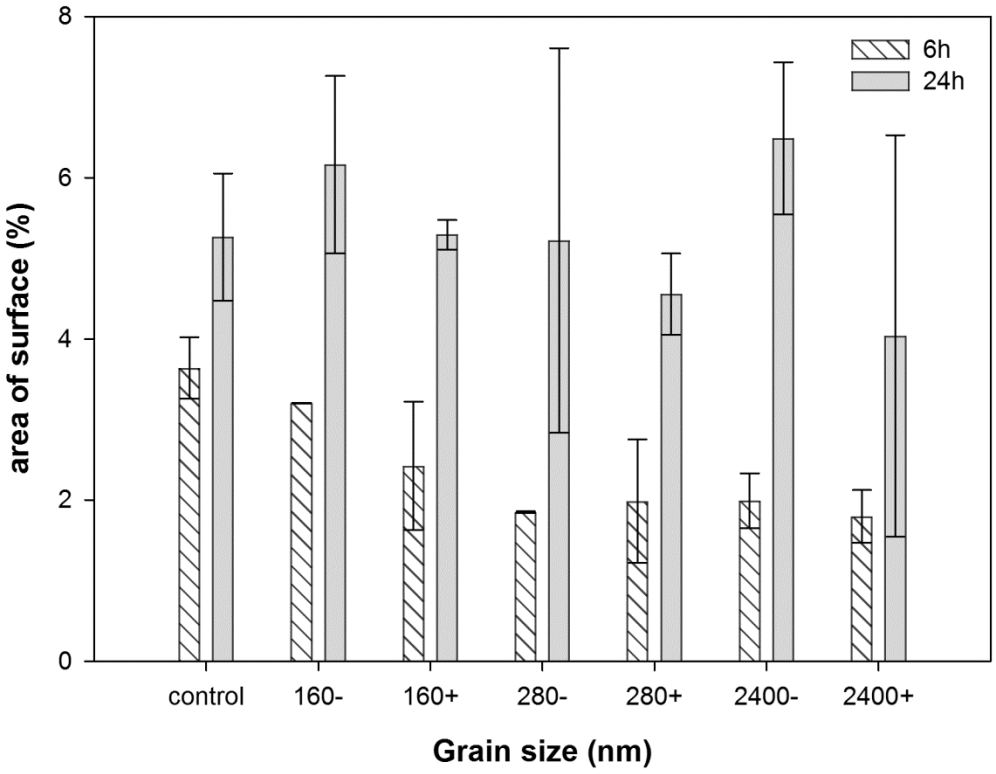

Figure 10: The area of surface (percentage) of six studied titanium materials with different rain sizes and sections occupied by human fibroblasts HFL1 at 6 hours and 4 hours after plating. Results from two distinct experiments on the basis of duplicate determination were combined. Error bars indicate means ± standard deviations.

Microscopic observation revealed that after 6 hours, fibroblasts presented a mainly rounded morphology (Figures 11a and 11c). After 24 hours the cells elongated and presented a mainly spindle-like structure. On the tissue culture plastic, we did not see any specific orientation (Figure 11d. However, on material samples the cells were aligned along concentric grooves (Figures 7b and 11b).

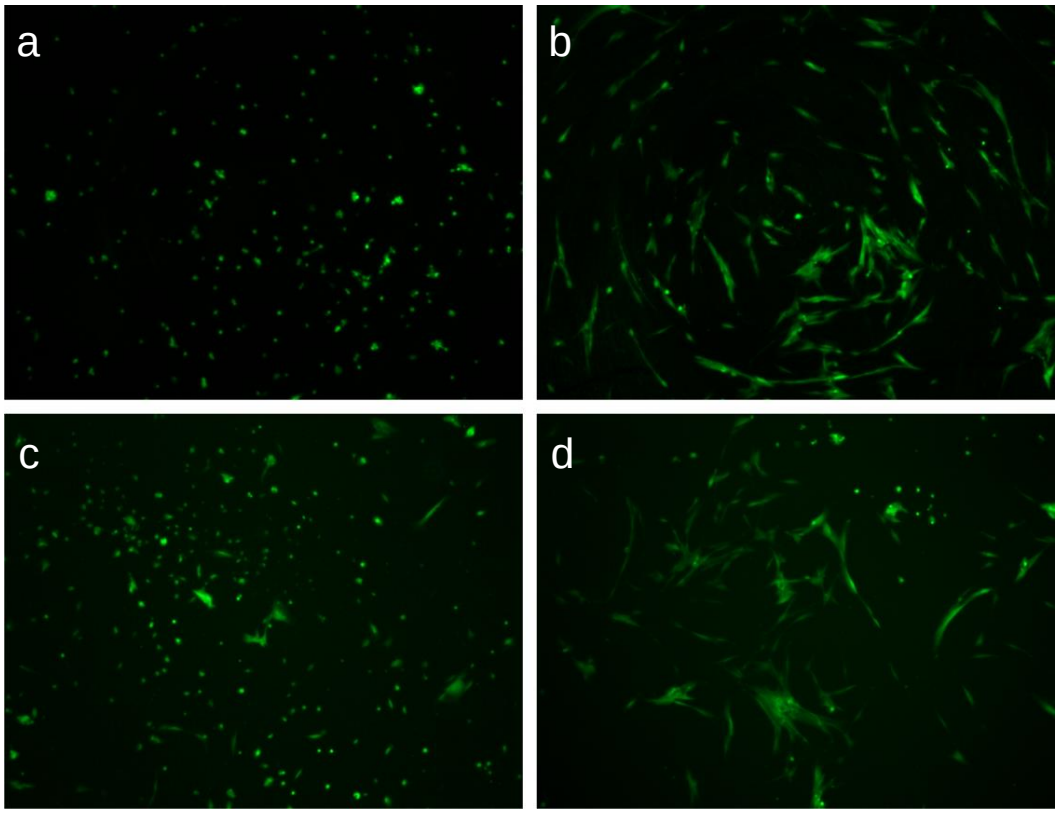

Figure 11: Fluorescence photographs of human fibroblasts HFL1 on tested titanium material (a, b) as well as control (c, d) at 6 hours (a, c) and 24 hours (b, d) after plating. 40x magnification.

MTT Assay

The viability of two cell lines (hFOB 1.19, HFL1) was estimated by MTT assay (Figure 12). The viability of fibroblasts growing on materials 160−, 280+, and 2,400+ was significantly lower than on control plates (P = 0.026). The osteoblast viability was lower, when growing on all types of studied titanium materials with the exception of 160+ material in comparison with the control ($P < 0.0001$).

The medians of viability of the cells (% of positive control) are shown in Table 6. We found higher viability of osteoblasts comparing materials 280− with 160+ and 2,400+ with 160+ (P = 0.0162, P = 0.0372; resp.). The comparison of other pairs of materials did not exhibit any significant differences.

On the other hand, material 160+ was a significantly better substrate for culturing osteoblasts than all other studied materials (P = 0.0072).

Material	Cross-section			Longitudinal section		
	160-	280-	2400-	160+	280+	2400+
hFOB 1.19	72.2	62.2	68.5	91.5	62.3	62.3
HFL1	68.1	71.4	77.5	77.8	71.5	73.4

Table 6: Medians of viability of two cell lines (hFOB 1.19, HFL1) estimated by MTT assay expressed as % of positive control.

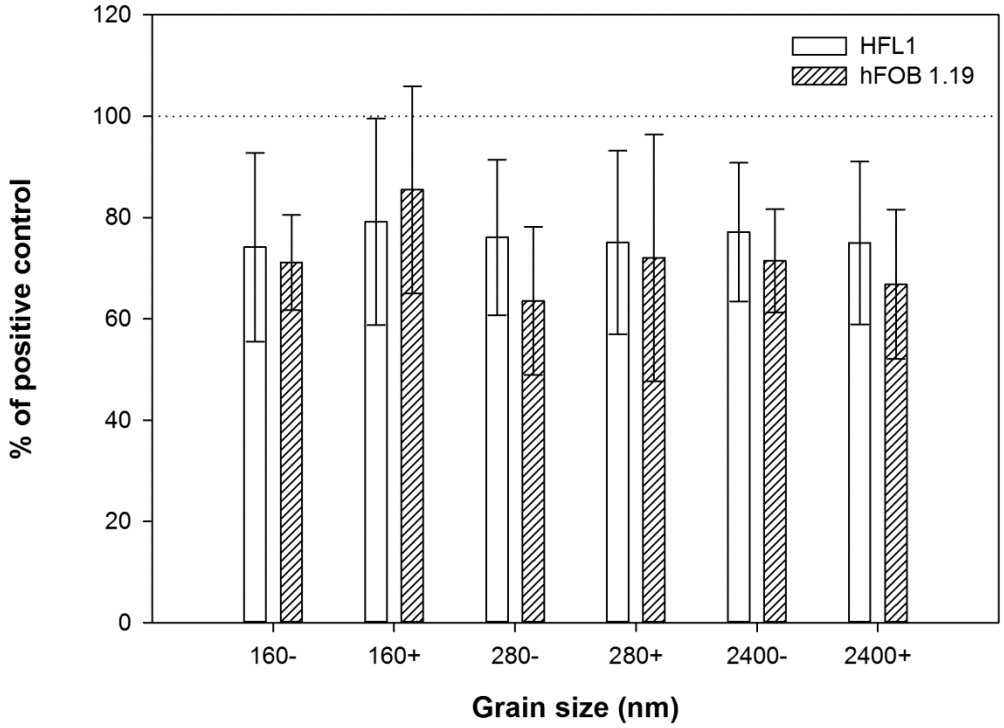

Figure 12: Comparison of the viability assessed by MTT assay of human fibroblasts HFL1 and human foetal osteoblast cell line, hFOB 1.19 grown on six studied titanium materials with different grain sizes. The standard errors were calculated from a combination of two independent experiments with quadruplicate measurements. Data expressed as % of positive control. Error bars indicate means ± standard deviations.

Immunocytochemistry

In order to compare morphology of the cytoskeleton, fibroblastic cells grown on the six different titanium materials underwent actin labelling with TRITC conjugated phalloidin and vinculin labelling with goat α-mouse Atto488 conjugated secondary antibody for mouse monoclonal anti-human vinculin antibody hVIN-1 (Figure 13).

Two hours after seeding, cytoskeleton analysis showed that cells presented a round shape and were not yet spread properly on the surfaces. On all tested materials, at this point of time, focal contacts could be seen as positive spots localised at the cellular edge.

After 48 hours, the cytoskeleton analysis mainly showed cells with an elongated bipolar morphology. On all tested surfaces, vinculin-positive focal contacts were present homogenously on the whole cell surface, with a slightly higher density at the cell periphery, at the ends of F-actin filaments. These data denote that the adhesion phase occurred on all tested materials.

3.1.7 Discussion

In our work, we examined how grain size of nanostructured titanium material influences the behaviour of fibroblastic as well as osteoblastic cells grown on its surface.

The grain size was shown to be an important factor that influenced not only the strength of material but also its interactions with cells. Kim et al. proved that the ultrafine grain titanium prepared by the ECAP method had better biocompatibility concerning wettability, cell adhesion, and proliferation of mouse fibroblasts. Our results did not clearly prove that grain size has a distinct impact on viability or proliferation of used fibroblast model (HFL1). The only differences we saw were related to the initial phase of attachment, but until 24 hours after seeding, differences almost disappeared. Faster cell attachment on material with the smallest grain size was observed.

The metabolic activity, assessed by MTT test, of the cells grown on 160−, 280+, and 2400+ titanium was significantly decreased against control. However, the tested materials did not differ among each other, which indicated that all tested materials were cytocompatible. This is in line with the numerous studies demonstrating the biocompatible character of titanium as a substrate for cell culturing.

The usage of a second cell model (hFOB 1.19) revealed that one of the tested materials seems to be as good as control with respect to metabolic activity of the osteoblasts cultured on its surface. It was the material with the smallest grain size that seemed to be consistent with the studies that detected that the smaller the grain size, the better the viability.

Other studied materials were significantly worse than control and 160+. Interestingly, this result was reached only for one of two materials with one certain grain size. This

observation indicated that two different sections differ in the viability of cells grown on its surface, which is in agreement with the study of Hoseini et al., who conclude that crystallographic texture, rather than grain size, plays a principal role in the surface biocompatibility.

It is well established that the proteins of extracellular matrix, membrane receptors, and cytoskeletal proteins are responsible for cell-substrate interactions. That is why we decided to analyse two important cytoskeletal proteins actin and vinculin by immunocytochemical staining. Actin is a critical player in many cellular functions, such as cell motility and the maintenance of cell shape and polarity. Vinculin is a cytoplasmic actin-binding protein enriched in focal adhesions and adherens junctions required for strong cell adhesion. As early as 2 hours after seeding, the cells adhered and began to spread (Figure 13a). The cells displayed well spreading morphology with many vinculin spots after 24 hours (Figure 13b). This observation proved that the adhesion phase occurred on all tested materials. We also intend to examine differences between two used cell models. Fibroblasts represent soft tissue and osteoblast hard tissue, and the dental implant needs to be in contact with both. We did not record significant differences in viability among tested materials plating with fibroblast cells. When we used osteoblasts as a cell model, we recorded that material with a grain size 160 nm with longitudinal section seemed to be as good as a conventional culture plate with respect to cell viability and proliferation. Therefore, this material could be recommended for a detailed study of cell behaviour *in vitro* as well as *in vivo*.

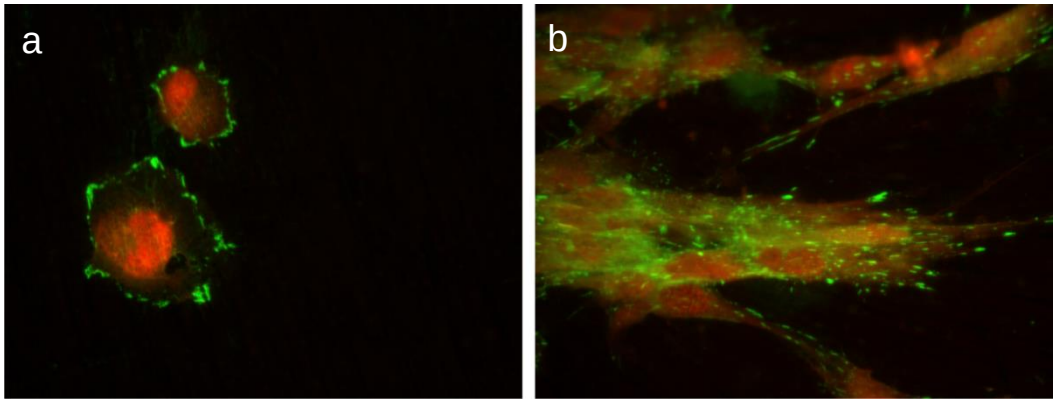

Figure 13: Visualisation of focal adhesion and cytoskeleton of human fibroblasts HFL1 on tested titanium material after 2 hours (a) and 48 hours (b) of seeding. Actin filaments (red), vinculin (green), 400x magnification.

3.2 Evaluating the Osseointegration of Nanostructured Titanium Implants in Animal Models

Animals of various species, size, and ages are used for the experimental evaluation of osseointegration. No species fulfils all requirements of an ideal model to determine an optimal interface between bone and dental implants. However, dog, sheep, goat, pig and rabbit models are commonly used to evaluate bone-implant interactions.

The dog seems to be more promising as animal model for testing bone implant materials, but there are increasing ethical issues relating to the use of dogs in medical research due to their status as companion animals.

With regard to bone anatomy, morphology, healing and remodelling, the pig demonstrates a good likeness to human bone. However, challenges may be encountered in relation to its large size and difficulty in handling. Currently, the development of miniature pigs has overcome these problems to some extent.

The rabbit is the most commonly used animal model. However, this species shows the fewest similarities to human bone, and its small size, which also limits the quantity and size of inserted implants, is a significant disadvantage.

The most common bones for implantation are a miniature pig maxilla and a rabbit femur. The most frequently used experimental animals, their age/weight (according to the primary literature), the bones selected for implantation, and healing time are shown in Table 7.

Animal	Age/weight of animal	Implantation site	Samples harvested after
Rabbit	approx. 4 kg	femur	3 weeks
	2.8-3.2 kg	nasal bone	8 weeks
	1-3 months/ 2.68±0.29 kg	femur	1 and 3 months
	6-8 months	femur	3 months
	3.0-3.5 kg	tibia	2 and 4 weeks
	4±1 kg	femur	6 and 12 weeks
Miniature pig	6 years	maxilla and mandible	4 and 6 weeks

	4 years/ 70-90 kg	maxilla	8 weeks
	2-4 years	maxilla	1, 2, 4 and 8 weeks
	1 year/ mean weight 60 kg	maxilla	4 and 8 weeks
Pig	18 months	calvaria	1, 2 and 4 weeks

Table 7: Animals, bones and healing time in recent studies on osseointegration of implants. As some of the studies do not provide details on animal age and size consistently, both values are included in the second column.

3.2.1 Titanium and Nanostructured Titanium

Titanium and its alloys are commonly used as biomaterials for both dental and orthopaedic implants due to their advantageous properties, including biocompatibility, nontoxicity, high specific strength, and corrosion resistance. Whilst commercially pure titanium has sufficient biocompatibility but relatively poor strength, titanium alloys have superior strength but contain potentially toxic or allergenic ingredients.

Because of their positive properties, such as the easy formation of a stable oxide, high corrosion resistance, and fast passivation, titanium and its alloys were among the first metals to be used for the manufacture of medical implants. The long-term stability of titanium implants depends on establishing direct bone-implant contact (BIC) without a fibrous connective tissue interface. Loosening or failure of the implant can be caused by inflammation and bone resorption induced by wear debris in the form of titanium particles from the implant that enter into the surrounding tissues. Therefore, it is essential to improve the biocompatibility and wear resistance of a titanium implant for its successful long-term survival.

3.2.2 Animal Species and Bones

Animals of various species, size, and ages are used for the experimental evaluation of osseointegration. No species fulfils all requirements of an ideal model to determine an optimal interface between bone and dental implants. However, dog, sheep, goat, pig and rabbit models are commonly used to evaluate bone-implant interactions.

The dog seems to be more promising as animal model for testing bone implant materials, but there are increasing ethical issues relating to the use of dogs in medical research due to their status as companion animals.

With regard to bone anatomy, morphology, healing and remodelling, the pig demonstrates a good likeness to human bone. However, challenges may be encountered in relation to its large size and difficulty in handling. Currently, the development of miniature pigs has overcome these problems to some extent.

The rabbit is the most commonly used animal model. However, this species shows the fewest similarities to human bone, and its small size, which also limits the quantity and size of inserted implants, is a significant disadvantage.

The most common bones for implantation are a miniature pig maxilla and a rabbit femur. The most frequently used experimental animals, their age/weight (according to the primary literature), the bones selected for implantation, and healing time are shown in Table 7.

3.2.3 Methods of Implantation into Compact and Spongy Bone

Selecting the target bone is an important step of the study design. For example, implants intended to be used in human maxilla may be tested in porcine maxilla. The maxilla has a variable layer of compact cortical bone on the surface, below which mostly spongy bone is found. However, both porcine and human mandibles have a substantially greater proportion of very thick compact bone. The average buccal cortical thicknesses are 1.69 mm (molar region), 1.43 mm (premolar region), and 1.04 mm (anterior region) in the edentulous maxilla and 2.06 mm (molar region), 1.78 mm (premolar region), and 1.36 mm (anterior region) in the edentulous mandible. Changes in the relative composition between trabecular and cortical bone in atrophic edentulous mandibles are due to loss of height and total area, mainly at the expense of trabecular bone, but not to changes in the cortical bone. Due to a different spatial organization of the compact and spongy bone, the choice of implant location might result in various values of the BIC parameter, which is the most widely used quantitative parameter for evaluating osseointegration (see below for details on BIC quantification). Moreover, different proximal vs. distal segments of long bones, such as the femur, tibia, and humerus (Table 7), may vary in the proportions of compact and spongy bones. Again, variable proportions of compact

and spongy bone tissue within the same anatomical bone could represent a possible source of bias. Whilst implants (or their parts) fully embedded within the compact bone could theoretically reach maximum values of BIC, parts of implants surrounded by spongy tissue will always be partially touching other types of tissue between the bone trabeculae, such as connective tissue or bone marrow. This will inevitably result in lower BIC parameter values. To prevent any significant bias, we suggest that studies on implant osseointegration should be accompanied by details on the ratio between compact and spongy bone at the site of implantation. Unfortunately, these values are rarely found in the literature. The cortical thickness of rabbit femoral proximal diaphysis is 9.5±0.4 mm.

3.2.4 ISO Standards in Implant Testing

The results of an experimental evaluation of osseointegration should be compatible with ISO Standards (ISO 10993-6 Biological evaluation of medical devices – Part 6: Tests for local effects after implantation), and several recommendations should be considered (ISO 10993-6, 2014) during the design of the experiment, as follows:

1) the diameter of the dental implant should be between 2 and 4.5 mm;
2) when using rabbit as an animal model, the maximum number of implants per animal is 6; and
3) when using a pig as a model, the number of implants per animal must not exceed 12.

3.2.5 *In Vivo* Evaluation

In an *in vivo* evaluation, animals are used to test the effect of various biological entities as well as to observe the overall effect of an experiment on a living subject. Under general anaesthesia and standard disinfection and aseptic conditions, skin incision and soft tissue preparation will be performed, and a mucoperiosteal flap will be incised and raised to expose the entire extent of the bone where the implants are to be placed. After bone exposure and surgical preparation of the bone, the implant will be inserted (Figure 14A) It is essential to use copious amounts of sterile saline irrigation and sharp drills to prevent heating the bone above 47 °C, which could result in bone cell death and osseointegration failure. The insertion technique depends largely on the implant system being used. Wounds will be closed primarily layer by layer from deep to superficial

tissue with resorbable suture material after thorough cleaning and irrigation. Following the surgical insertion of an implant in the animal and post-operative care, the animal is allowed to mature and will then be sacrificed. During the period of healing and osseointegration, it is possible to perform radiographic examinations, such as X-ray, CT or densitometry analysis, to track the healing progress and determine the exact position of the implants (Figure 14B) After sacrificing the animal and separating the bone containing the implants from the soft tissue, other radiographic images will be taken for analysis (Figure 14C).

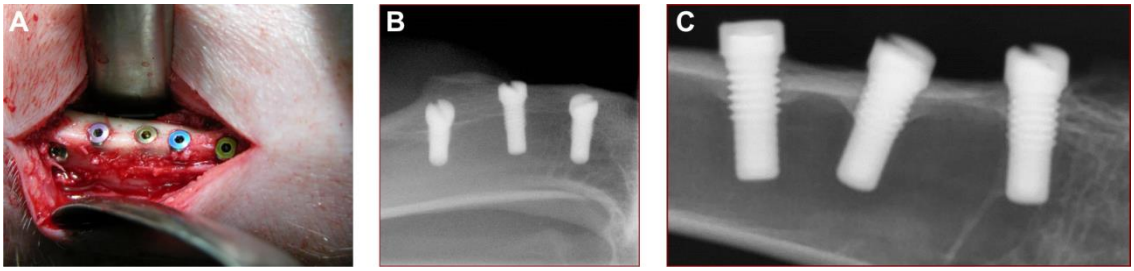

Figure 14: A – Implants inserted into the pig mandible, B – X-ray of rabbit femur 2 weeks after surgery, C – X-ray of rabbit femur 12 weeks after surgery (shortly after the animal has been euthanized).

In general, handling wild animals during experiments is difficult, and complications may occur at any time. At the time of surgery, the animal can be lost due to the introduction of intratracheal intubation during general anaesthesia. Infection of the wound, which is a common postoperative complication, may develop because maintaining animals in a hygienic environment is extremely challenging (Figure 15A,B,C). Based on our experience, the utilization of young animals for experiments may bring another complication. Radiographic images have revealed the occurrence of opposition of bone above the implant head due to osteoblastic activity, and the largest part of the implant shifted inside the bone marrow cavity due to the osteoclastic activity of osteoclasts. This led to resorption of bone at the distal part of implant because of the rapid growth of the animal.

Figure 15: Postoperative inflammatory complication (A – Rejected implant due to inflammation, B – rejected implant after explantation, C – X-ray of inflamed bone).

3.2.6 Histologic Processing of Implants

3.2.6.1 Harvesting the Samples

At the end of the experiment, tissue samples are harvested from the animals and processed. The anatomical position and orientation of implants in bone should be verified using X-rays. This is also very helpful for subsequent cutting of bones into smaller tissue blocks of bone with implants. A suitable tissue-block size for histological processing depends on the size of the implants or the size of formed defects during the evaluation of degradable osteoinductive biomaterial. The tissue block should be as small as possible for better penetration of fixation fluid. However, at least two millimetres of bone tissue surrounding the implant should be preserved to allow for a reliable evaluation of osseointegration. Therefore, tissue blocks exceeding 2×2×2 cm are cut using either a diamond band saw (Figure 16A) or a special low speed diamond wheel saw. The orientation of the tissue blocks relative to the original anatomical positions should be marked and carefully maintained during all processing steps. Further processing might differ in samples of surrounding bone without implants (in this case, the samples may be decalcified), or in samples with implants (undemineralized samples).

3.2.6.2 Undemineralized Ground Sections

There are methods for processing hard tissue, and for the evaluation of osseointegration of titanium implants, a resin and cutting-grinding system is suitable. This method provides information on the formation and mineralization of a new bone matrix adjacent to the implant.

Fixation and Dehydration

The time of fixation in a 10% formaldehyde solution depends on the sample thickness. Tissue blocks 2-4 mm thick require approximately 12 hours for penetration. Slightly thicker samples require approximately 24 hours, but some researchers recommend up to 5 days for 16 mm thick samples. An important factor affecting the fixation time is the ratio of spongy bone (with relatively easy fixation) to compact bone (which requires a longer fixation time). The samples are then dehydrated in ascending grades of alcohol of 70%, 80%, 96%, and 100% (two days required per grade of alcohol). After the 100% alcohol treatment, the samples are transferred to a 1:1

Embedding

Methacrylate-based resins are currently the most commonly used embedding media. The time required for dehydration and saturation by resin can be shortened using an automatic embedding device with an agitation and vacuum system. The samples are put in methyl methacrylate (MMA) without an initiator of polymerization for approximately four days. The samples are then put in a mould with resin, and the polymerization of resin is initiated either by blue/ultraviolet light or peroxide. A plastic block is formed (Figure 16B). Another resin frequently used for embedding is epoxy resin (e.g., Epon). When using epoxy-based embedding resins, after dehydration, the samples are put into 100% propylene oxide twice for 15 minutes, followed by a 1:1 mixture of propylene oxide and Epon overnight and then into clean Epon for two days at 37 °C. Verifying the position of an implant in a plastic block with an X-ray might be necessary in non-transparent resins.

Sectioning

The blocks of samples are sectioned along the long axis in the middle of the implants to form two blocks. The sample can be cut with a diamond saw band (Exact Apparatebau, Norderstedt, Germany), a diamond disc (Figure 16C) (Struers, Ballerup, Hovedstaden, Denmark) or a special saw microtome. The cutting area is ground by P1200 grit sandpaper until the all tissue segments for observation are exposed to the surface. After grinding, the cutting area is polished with P4000 grit sandpaper. A clean slide is glued to the polished side. The second incision is made approximately 100-300 μm from and parallel to the slide.

Grinding and Polishing

The slide with the section is ground using a sequence of abrasive papers (P320, P1200 and P2500 grit) and polished using P4000 grit sandpaper under water irrigation to a final thickness of approximately 50-30 µm. For the final polishing of the surface paper coated with a fine cloth and diamond paste with grain roughness 3 µm are used. The papers for grinding and polishing are on a rotating desk and the samples are pressed towards the desk.

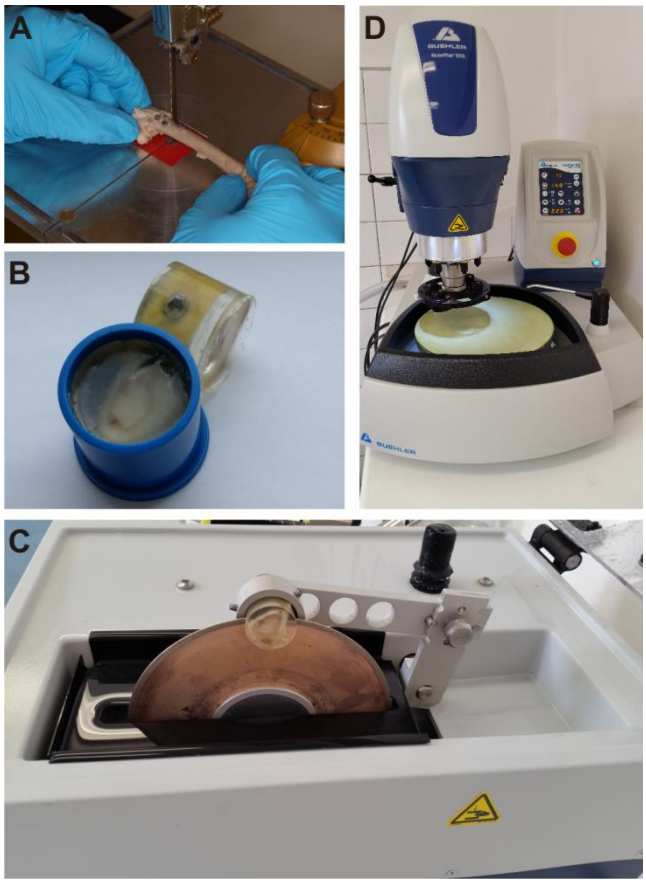

Figure 16: Processing of samples (A – Formation of tissue blocks using diamond saw band, B – formation of resin blocks, C – diamond disk used for cutting of titanium implants along its long axis, D – grinding and polishing of samples).

Staining

The most commonly used staining method is toluidine blue (Figure 17A). Toluidine blue can easily differentiate unmineralized osteoid from fully mineralized bone tissue and provides sufficient preservation of morphological details. Basic fuchsine can be

used alone (Figure 17C) for staining microporous bone or can be combined with toluidine blue. Other staining methods for MMA-embedded samples are shown in Table 8.

MMA-embedded sections can also be stained by immunohistochemistry as described in decalcified sections. The sections have to undergo dissolution of the embedding resin using 2-methoxyethyl acetate for 24 hours and are then cleaned with ethanol, rehydrated using a descending ethanol series, and transferred into distilled water. MMA-embedded non-decalcified bone yields a stronger immunostaining reaction compared to decalcified bone embedded in paraffin. There is also better preservation of the trabecular bone morphology.

Stain	Nuclei	Unmineralized osteoid	Mineralized bone	Cartilage
Haematoxylin and eosin	blue	pink	purplish brown	
von Kossa method	red	red	black	dark brown
Goldner′s trichrome method	blue-grey	orange-red	green	purple
Toluidine blue	blue	sky blue	light purple	purple
Levai-Laczko	violet blue		bright red	light blue

Table 8: Staining methods and their results in ground sections.

3.2.6.3 Demineralized (Decalcified) Histological Sections

Alternatively, bone samples without metal implants, such as biopsies of bone tissue or bone from the regions between the implantation sites, may undergo demineralization. This technique may be beneficial for the evaluation of degradable osteoinductive biomaterials because it demonstrates organic components of bone, such as osteocalcin;

(Figure 17B,E); osteopontin; and type I collagen (Figure 17D). After using a decalcification solution, the samples may be processed using a routine histological paraffin-embedding technique. The most common decalcifying solution is the neutral ethylenediaminetetraacetic (EDTA) acid. Decalcification time depends on the sample size. Because the demineralization in EDTA requires approximately 8-10 weeks, alternative solutions of acids may be used to accelerate the process. However, some of the more aggressive decalcifying solutions, such as formic acid, may damage the structure of the tissue, thereby limiting its further evaluation. Moreover, some biomaterials are harder than bone and have to remain in a decalcification solution for a longer period of time. This can affect the morphology of bone, its dyeability and the next evaluation. Unfortunately, osteoinductive materials, such as hydroxyapatite granules, may affect the cutting of samples because the material can be harder than bone and needs to remain in the decalcification solution for a longer period of time. Some hard particles of biomaterial can fall out during sectioning.

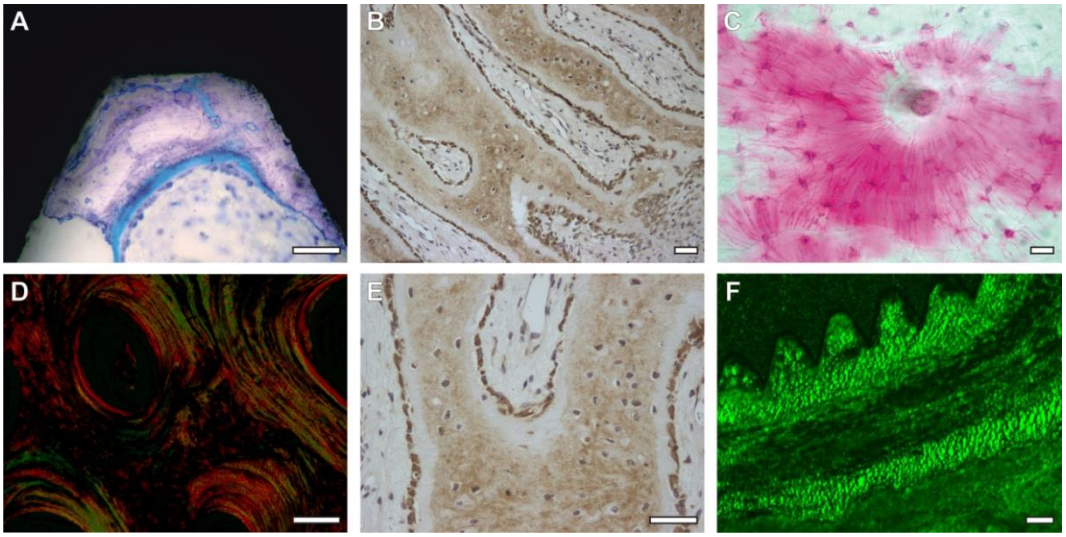

Figure 17: Staining methods for bone samples evaluation. A – Sky blue osteoid on the surface of bone trabeculae adjacent to titanium implant (toluidine blue stain), B – brown osteocalcin in osteoblasts and ECM on decalcified section (anti-osteocalcin antibody OCG3 visualized by diaminobenzidine), C – pink blood vessels and osteocyte lacunae in bone (basic fuchsine stain), D – red or yellow type I collagen in ECM and green type III collagen (picrosirius red stain, polarized light), E – detail of osteocalcin staining, F – tetracycline incorporated into newly formed bone visualized as a strong

green fluorescence signal; the distance between the two outlines of fluorescence is proportional to the bone newly built between the two administrations of tetracycline (double tetracycline labelling, confocal fluorescence microscope).

3.2.7 Microscopic Evaluation

Qualitative Evaluation

Using the staining methods shown in Table 8, qualitative findings, such as the formation of unmineralized osteoid and mineralized tissue, loose connective tissue surrounding the implant surface, or the formation of granuloma with excessive vascularization but poor mechanical retention, can be obtained.

Histological Quantification of Bone-Implant Contact

Quantitative histological techniques are frequently used to demonstrate which part of the bone directly binds to fully differentiated bone tissue. The most commonly used quantitative parameter for the evaluation of osseointegration is the bone-implant contact (BIC), which is expressed as follows:

$$\mathrm{BIC} = \frac{BC}{IL}, \tag{1}$$

where bone contact (BC) refers to the length of direct contact between the implant profile and bone tissue, and interface length (IL) indicates the total length of the implant surface projected to the section plane. The BIC is a continuous variable expressed as a dimensionless ratio of <0;1>, where BIC=0 denotes no direct contact between implant and bone, and BIC=1 theoretically means that the entire implant is fully embedded within the bone tissue. Alternatively, BIC is often expressed as a percentage value. When quantifying objects of macroscopic size (such as the implant-bone interface) on a microscopic scale, an appropriate and unbiased sampling of the microscopic fields of view from the entire object has to be performed. Briefly, all parts of the specimen should be given the same chance to be sampled with the microscopic fields of view and included in the quantification. Selecting a lower objective magnification results in a larger field of view but a poor differentiation of the bone-implant interface details. Therefore, the magnification should be adjusted according to the amount of detail in a

particular study so that an unambiguous identification of that detail is possible. Either all the adjacent microscopic fields of view are included (Figure 18A) or for larger implants, a systematic uniform sampling of the objective image fields is performed by selecting, for example, every second field of view (Figure 18B).

Delineating the BC and IL lines could be done manually. Alternatively, stereological grids and principles of stochastic geometry may be used for this task as follows:

1) a two-dimensional system of lines with known geometrical properties is randomly positioned over the series of calibrated micrographs sampled from the bone-implant interface (Figure 18B). The line system consisting of perpendicular equidistant lines with randomized orientation is isotropic, i.e., it has the same geometrical properties in all directions and does not favour any direction.
2) The number of intersections between the line system and the profile of the implant surface is counted manually. According to the modified stereological Buffon's method, the total number of intersections (orange points in Figure 18C,D) is directly proportional to the IL, i.e., implants with more structured and greater surface will have more intersections with the testing grid.
3) By contrast, the number of intersections hitting the profile of the implant surface attached to the bone is counted. Again, the total number of these intersections (light blue points in Figure 18B) is proportional to the BC. After summing all BC and IL points from all microscopic image fields from the same specimen, an average BIC value may be calculated as the BC/IL ratio. The total number of points hitting the profile of the implant surface should be a minimum of 150. Based on our experience, this stereological method is highly reproducible, gives consistent results, does not require calibration, is easy to learn and is robust to any possible histological artefacts.

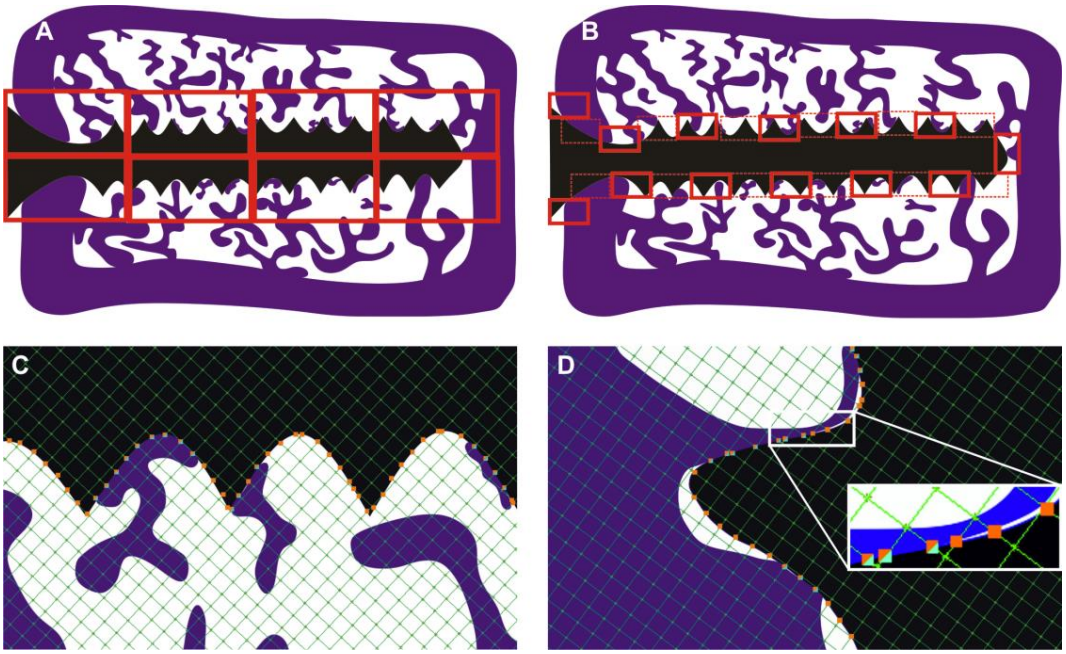

Figure 18: Stereological quantification of the bone-implant contact. A – Sampling of image fields (red squares) using a low microscope magnification; all adjacent fields showing the implant surface (black) and bone (purple) are taken, B – alternatively, every second image field is sampled; especially used when higher magnification with small field of view is needed, C – stereological grid randomly positioned over the micrograph; intersections between the test lines and the implant surface (orange points) and intersections between the implant-bone interface and test lines (light blue points), D – the same way evaluation but using a higher magnification; detail of BIC and the testing grid is shown in embedded rectangle (the bone has blue colour).

Histological Quantification of Other Bone Characteristics

Vascularization of the bone adjacent to the implant and the numerical density of osteocyte lacunae within the bone may be assessed using the stereological point-counting technique. The lacunar microporosities (density of osteocytes) may be statistically independent from the vascular microporosities (bone vascularization), and therefore, both parameters should be regarded as complementary characteristics of bone quality.

Alternatively, the amount of bone tissue formed within a certain time interval in the region used for implantation may be quantified using the tetracycline labelling test. Briefly, a tetracycline antibiotic is administered at two time points. Due to its relatively

short biological half-time but high affinity to the bone tissue, tetracycline incorporates into bone tissue formed within a specific period, i.e., 1 to 2 days after administration. Using the autofluorescence of the tetracycline the bone formed between the two administrations of tetracycline can be visualized using fluorescence microscopy of the ground sections (Figure 17F). The width of the bone region between the two lines marked with tetracycline is proportional to the bone that forms between the two administrations of tetracycline.

3.2.8 Results and Discussion

Based on results of our experiments, we can conclude that the surface of the implant plays a very important role in osseointegration and that mechanically added surface roughness significantly increases the contact area between the implant surface and the peri-implant bone. It is important to note that there are many physiological and pathological influences that can affect the results, and it is vital to repeat the method several times to increase the accuracy of the results.

Implant technology is a rapidly progressing science with frequent production of new designs, materials, shapes and surface treatments. Therefore, based on the success of our method, we could utilize this method in the future to analyse these new modifications. The current method that was used made the evaluation of osseointegration more efficient, more accurate and faster. An important area of research involves the creation of a 'biomimetic surface', or a surface that closely resembles that of real tissue, which would assist in the stimulation and proliferation of bone tissue because it stimulates the regularity and dimensions of the bone tissue itself without altering the properties of titanium.

To perform a similar experiment, older animals or miniature pigs that have a slower rate of growth are recommended. A histological evaluation of experimental osseointegration of dental implants requires a careful choice of experimental animals, bones, and implantation sites. Bones with a similar ratio of compact to spongy bone, such as the human maxilla and mandible, are preferred. Quantification of the BIC contact may be performed using an unbiased stereological method, but an appropriate and fair sampling of the microscopic image fields is an absolute prerequisite of the quantification procedure.

The successful outcome of any implant procedure is mainly dependent on the interrelationship of the various components of an equation that includes the following:

1) Biocompatibility of the implant material,
2) macroscopic and microscopic nature of the implant surface and designs,
3) the status of the implant bed in both a health and a morphologic (bone quality) context,
4) the surgical technique itself,
5) the undisturbed healing phase,
6) loading conditions.

The challenge confronting the clinician is that these several factors must be controlled almost simultaneously, if a predictably successful outcome is to be expected.

In conclusion, histological evaluation of the experimental osseointegration of dental implants requires careful selection of the experimental animals, bones, and implantation sites. It is also advisable to use larger animal models and older animals with a slower growth rate rather than small or growing experimental animals. Bones with a similar ratio of compact to spongy bone, such as the human maxilla and mandible, are preferred.

4 Summary

In the first experiment, similar cellular behaviour was observed on all studied biomaterials. There were differences related to the initial phase of attachment, but not in proliferation.

Furthermore, the results indicate that osteoblasts grow on material with a grain size of 160 nm with longitudinal section as well as on a conventional culture plate, whereas, for other studied materials, we observed decreased viability. This material could be recommended for further evaluation with respect to osseointegration *in vivo*.

It was proven all tested materials were cytocompatible and that grain size influences strength of material as well as its interactions with cells – the smaller grains, the better biocompatibility and cell viability.

Different sections did not significantly differ in viability of cells grown on its surface – crystallographic texture is more important than grain sizes - the only differences observed were related to the initial phase of attachment, but until 24 hours after seeding, differences almost disappeared.

The second study reviewed current methods used in the experimental evaluation of the osseointegration of dental implants. The results of histological staining methods used in implantology were illustrated and compared. A standardized and reproducible technique for stereological quantification of bone-implant contact was proposed and demonstrated.

It was verified that surface modifications play a very important role in biocompatibility and osseointegration and that mechanically added surface roughness significantly increases the contact area between the implant surface and the peri-implant bone.

5 References

1. Ring, ME. *Dentistry: An Illustrated History*. 2nd ed. Abradale Press, New York, 1985. ISBN 9780810911000.
2. Brånemark PI, Adell R, Breine U, et al. Intra-osseous anchorage of dental prostheses: I. Experimental studies. *Scand J Plast Reconstr Surg Hand Surg* (1969), **3**(2): 81-100.
3. Wang W, Liao S, Zhu Y, et al. Recent Applications of Nanomaterials in Prosthodontics. Review article. *J Nanomater* (2015), Article ID 408643, 11 pages. DOI 10.1155/2015/408643.
4. Esposito M, Hirsch JM, Lekholm U, and Thomsen P. Biological factors contributing to failures of osseointegrated oral implants. (I). Success criteria and epidemiology. *Eur J Oral Sci* (1998), **106**(1): 527-551.
5. Osborn JF, Newesely H. The material science of calcium phosphate ceramic. *Biomaterials* (1980); **1**(2): 108–111.
6. LeGeros RZ, and Craig RG. Strategies to affect bone remodeling: Osseointegration. *J Bone Miner Res* (1993); **8**(Suppl. 2): S583–S596. DOI: 10.1002/jbmr.5650081328.
7. Sykaras N, Iacopino AM, Marker VA, Triplett RG, and Woody RD. Implant materials, designs, and surface topographies: their effect on osseointegration. A literature review. *Int J Oral Maxillofac Implants* (2000), **15**(5): 675–690. ISSN 0882-2786.
8. Ellingsen JE, Thomsen P, and Lyngstadaas SP. Advances in dental implant materials and tissue regeneration. *Periodontology* (2000), **41**(1): 136–156. doi:10.1111/j.1600-0757.2006.00175.x
9. Ananth H, Kundapur V, Mohammed HS, et al. A review on biomaterials in dental implantology. *Int J Biomed Sci* (2015); **11**(3), p. 113-120. ISSN 1550-9702.
10. McCracken M. Dental implant materials: commercially pure titanium and titanium alloys. *J Prosthodont* (1999), 8(1): 40-43. ISSN*:* 1059-941X.
11. Wataha JC. Materials for endosseous dental implants. *J Oral Rehabil* (1996), **23**(2): 79-90. ISSN 0305-182X.

12. Valiev RZ, Kaibyshev OA, Kuznetsov RI, Musalimov RS, and Tsenev NK. Low-temperature superplasticity of metallic materials. *Proceedings of the Academy of Sciences of the USSR* (1988), **301**(4): 864-866.
13. Valiev RZ, Krasilnikov NA, and Tsenev NK. Plastic deformation of alloys with submicron-grained structure. *Mater Sci Eng A* (1991), 137: 35–40. DOI: 10.1016/0921-5093(91)90316-F.
14. Valiev RZ, Islamgaliev RK, and Alexandrov IV. Bulk nanostructured materials from severe plastic deformation. *Prog Mater Sci* (2000), **45**(2): 103-189. DOI: 10.1016/S0079-6425(99)00007-9.
15. Petruželka, Dluhoš L, Hrušák D, and Sochová J. Nanostructured titan – a new material for dental implants. *Čes Stomat* (2006), **106**(3): 72-77. ISSN 1213-0613.
16. Valiev RZ, Semenova IP, Latysh VV, et al. Nanostructured titanium for biomedical applications. *Adv Eng Mater* (2008), **10**(8): B15-B17. DOI: 10.1002/adem.200800026.
17. Furukawa M, Horita Z, Nemoto M, and Langdon TG. Processing of metals by equal-channel angular pressing. *J Mater Sci* (2001), **36**(12): 2835-2843.
18. Hrušák D, Zemko M, Dluhoš L, and Kraus L. Usage of nanostructured titanium for endosteal implants. In: *Proceedings of the 1st Conference with International Participation Nanocon (Oct 2009), S1B3, Rožnov pod Radhoštěm 2009, Czech Republic.*
19. Webster TJ, Siegel RW, and Bizios R. Osteoblast adhesion on nanophase ceramics. *Biomaterials* (1999), **20**(13): 1221-1227. DOI: 10.1016/S0142-9612(99)00020-4.
20. Tran N, and Webster TJ. Nanotechnology for bone materials. *Wiley Interdiscip Rev Nanomed Nanobiotechnol (*2009), **1**(3): 336-351. DOI: 10.1002/wnan.23.
21. Balasundaram G, and Webster TJ. A perspective on nanophase materials for orthopedic implant applications. *J Mater Chem* (2006), **16**(38): 3737-3745. DOI: 10.1039/B604966B.
22. Variola F, Vetrone F, Richert L, et al. Improving biocompatibility of implantable metals by nanoscale modification of surfaces: an overview of strategies, fabrication methods, and challenges. *Small* (2009), **5**(9): 996-1006. DOI: 10.1002/smll.200801186.

23. Dalby MJ, Gadegaard N, Tare R, et al. The control of human mesenchymal cell differentiation using nanoscale symmetry and disorder. *Nat Mater* (2007), **6**(12): 997-1003. DOI: 10.1038/nmat2013.
24. Oh S, Brammer KS, Li YSJ, et al. Stem cell fate dictated solely by altered nanotube dimension. *Proc Natl Acad Sci U S A* (2009), **106**(7): 2130-2135.
25. Bertoncini P, Le Chevalier S, Lavenus S, Layrolle P, and Louarn G. Early adhesion of human mesenchymal stem cells on TiO_2 surfaces studied by single-cell force spectroscopy measurements. *J Mol Recognit* (2012), **25**(5): 262-269. DOI: 10.1002/jmr.2193.
26. Jemat A, Ghazali MJ, Razali M, and Otsuka Y. Surface Modifications and Their Effects on Titanium Dental Implants. *Biomed Res Int* (2015). Article ID 791725, 11 pages, 2015. DOI: 10.1155/2015/79172.
27. Boyan BD, Hummert TW, Dean DD, and Schwartz Z. Role of material surfaces in regulating bone and cartilage cell response. *Biomaterials* (1996), **17**(2): 137-146. DOI: 10.1016/0142-9612(96)85758-9.
28. Chauvy PF, Madore C, and Landolt D. Variable length scale analysis of surface topography: Characterization of titanium surfaces for biomedical applications. *Surf Coat Technol* (1998), 110: 48-56. DOI: 10.1016/S0257-8972(98)00608-2.
29. Hsiao WT, Chang HC, Nanci A, and Durand R. Surface microtexturing of Ti–6Al–4V using an ultraviolet laser system. *Mater Des* (2016), **90**: 891-895.
30. Dumas V, et al. Femtosecond laser nano/micro patterning of titanium influences mesenchymal stem cell adhesion and commitment. *Biomed Mater* (2015), **10**(5): 055002.
31. Hindy, A., Farahmand, F., and Tabatabaei, F. In vitro biological outcome of laser application for modification or processing of titanium dental implants. *Lasers Med Sci* (2017) **32**(5): 1197-1206. DOI: 10.1007/s10103-017-2217-7.
32. Kim H, Choi SH, Ryu JJ, et al. The biocompatibility of SLA-treated titanium implants. *Biomed Mater* (2008); **3**(2). DOI: 10.1088/1748-6041/3/2/025011.
33. Davies JE. Mechanisms of endosseous integration. *Int J Prosthodont* (1998), **11**(5): 391-401.
34. Kim JH, Lee MA, Han GJ, and Cho BH. Plasma in dentistry: a review of basic concepts and applications in dentistry. *Acta Odontol Scand* (2014), **72**(1): 1-12.

35. Buser D, Schenk RK, Steinemann S, Fiorellini JP, Fox C, and Stich H. Influence of surface characteristics on bone integration of titanium implants. A histomorphometric study in miniature pigs. *J Biomed Mater Res* (1991), **25**(7), 889-902.
36. Ban S, Maruno S, Arimoto N, Harada A, and Hasegawa J. Effect of electrochemically deposited apatite coating on bonding of bone to the HA-G-Ti composite and titanium. *J Biomed Mater Res* (1997), **36**(1): 9-15.
37. Yang CY, Wang BC, Lee TM, Chang E, and Chang GL. Intramedullary implant of plasma-sprayed hydroxyapatite coating: an interface study. *J Biomed Mater Res* (1997), **36**(1): 39-48.
38. Baleani M, Viceconti M, and Toni A. The effect of sandblasting treatment on endurance properties of titanium alloy hip prostheses. *Artif Organs* (2000), **24**(4): 296-299.
39. Wennerberg A, Hallgren C, Johansson C, and Danelli S. A histomorphometric evaluation of screw-shaped implants each prepared with two surface roughnesses. *Clin Oral Implant Res* (1998), **9**(1): 11-19.
40. Wennerberg A, Albrektsson T, and Lausmaa J. Torque and histomorphometric evaluation of c.p. titanium screws blasted with 25- and 75-microns-sized particles of Al_2O_3. *J Biomed Mater Res* (1996), **30**(2): 251-260.
41. Zinger O., Anselme K., Denzer A. et al. Time-dependent morphology and adhesion of osteoblastic cells on titanium model surfaces featuring scale-resolved topography. *Biomaterials*, 2004; **25**(14): 2695-2711.
42. Smeets R., Stadlinger B., Schwarz F. et al. Impact of dental implant surface modifications on osseointegration. *Biomed Res Int* (2016). Article ID 6285620, 16 pages, 2016. doi:10.1155/2016/6285620.
43. Bullis G, Shah S. Implant Surface Treatments. A Literature Review. *Inclusive*, **5**(2): 87-89.
44. Sartoretto SC, Alves ATNN, Resende RFB, et al. Early osseointegration driven by the surface chemistry and wettability of dental implants. *J Appl Oral Sci* (2015), **23**(3): 279-287. DOI: 10.1590/1678-775720140483.
45. Stefan K. Roehling SK, Meng B, and Cochran DL. Sandblasted and acid-etched implant surfaces with or without high surface free energy: Experimental and clinical background. In: *Wennerberg A, Albrektsson T, and Jimbo R (Eds). Implant*

surfaces and their biological and clinical impact. Springer Verlag Berlin Heidelberg: 93-136. ISBN: 978-3-662-45378-0.

46. Choi AH, Ben-Nissan B, Matinlinna JP, and Conway RC. Current perspectives: calcium phosphate nanocoatings and nanocomposite coatings in dentistry. *J Dent Res* (2013), **92**(10): 853–859.
47. Marco F, Milena F, Gianluca G, and Vittoria O. Peri-implant osteogenesis in health and osteoporosis. *Micron* (2005), **36**(7-8): 630–644.
48. Abraham CM. A brief historical perspective on dental implants, their surface coatings and treatments. *Open Dent J* (2014), **8**(1): 50–55.
49. Trisi P, Keith DJ, and Rocco S. Human histologic and histomorphometric analyses of hydroxyapatite-coated implants after 10 years of function: a case report. *Int J Oral Maxillofac* Implants (2005), **20**(1): 124–130.
50. Albrektsson T. Hydroxyapatite-coated implants: a case against their use. *J Oral Maxillofac Surg* (1998), **56**(11): 1312–1326.
51. Esposito M, Dojcinovic I, Germon L, et al. Safety and efficacy of a biomimetic monolayer of permanently bound multi-phosphonic acid molecules on dental implants: 1 year post-loading results from a pilot quadruple-blinded randomised controlled trial. *Eur J Oral Implantol* (2013), **6**(3): 227–236.
52. Bonfante EA, Granato R, Marin C, et al. Biomechanical testing of microblasted, acid-etched/microblasted, anodized, and discrete crystalline deposition surfaces: an experimental study in beagle dogs. *Int J Oral Maxillofac Implants* (2013), **28**(1): 136-142.
53. Terheyden H, Lang NP, Bierbaum S, Stadlinger B. Osseointegration—communication of cells. *Clin Oral Implants Res* (2012), **23**(10): 1127–1135. doi: 10.1111/j.1600-0501.2011.02327.x.
54. Junker R, Dimakis A, Thoneick M, Jansen JA. Effects of implant surface coatings and composition on bone integration: a systematic review. *Clin Oral Implants Res* (2009), **20**(supplement 4): 185–206. doi: 10.1111/j.1600-0501.2009.01777.x.
55. Carreira AC, Lojudice FH, Halcsik E, Navarro RD, Sogayar MC, Granjeiro JM. Bone morphogenetic proteins: facts, challenges, and future perspectives. *J Dent* Res (2014), **93**(4): 335–345. doi: 10.1177/0022034513518561.

56. De Barros RRM, Novaes AB, Korn P, et al. Bone formation in a local defect around dental implants coated with extracellular matrix components. *Clin Implant Dent Relat Res* (2015), **17**(4): 742–757. doi: 10.1111/cid.12179.
57. Broggini N, Tosatti S, Ferguson SJ, et al. Evaluation of chemically modified SLA implants (modSLA) biofunctionalized with integrin (RGD)- and heparin (KRSR)-binding peptides. *J Biomed Mater Res A* (2012) **100**(3): 703-711. DOI: 10.1002/jbm.a.34004.
58. Compton JT, Lee FY. A review of osteocyte function and the emerging importance of sclerostin. *J Bone Joint Surg Am Title* (2014), **96**(19): 1659–1668. doi: 10.2106/jbjs.m.01096.
59. Peter B, Pioletti DP, Laib S, et al. Calcium phosphate drug delivery system: influence of local zoledronate release on bone implant osteointegration. *Bone* (2005), **36**(1): 52–60.
60. Stadlinger B, Lode AT, Eckelt U, et al. Surface-conditioned dental implants: an animal study on bone formation. *J Clin Periodontol* (2009), **36**(10): 882–891.
61. Xuereb M, Camilleri J., and Attard N. Systematic review of current dental implant coating materials and novel coating techniques. *Int J Prosthodont* (2015), **28**(1): 51-59 [cit. 2017-06-24]. DOI: 10.11607/ijp.4124. ISSN 08932174.
62. Edited by Sakaguchi RL, and Powers JM. *Craig's restorative dental materials*. 13th ed. Philadelphia, PA: Elsevier/Mosby, 2012. ISBN 9780323081085.
63. Schmalz G, and Garhammer P. Biological interactions of dental cast alloys with oral tissues. *Dent Mater* (2002), **18**(5): 396-406.
64. Harris SA, Enger RJ, Riggs BL, and Spelsberg TC. Development and characterization of a conditionally immortalized human fetal osteoblastic cell line. *J Bone Miner Res* (1995), **10**(2): 178-186.
65. YD, Choi HJ, Lee H, et al. Cellular viability and genetic expression of human gingival fibroblasts to zirconia with enamel matrix derivative (Emdogain®). *J Adv* Prosthodont (2014), **6**(5): 406-414.
66. Gristina A. (2004). Biomaterial-centered infection: Microbial adhesion versus tissue integration. *Science* (1987), **237**(4822): 1588-1595.
67. Sitbon YAD. Epithelial cells attachment on five different dental implant abutment surface candidates. Master of Science Thesis, The University of Iowa, 2009. Available from: http://ir.uiowa.edu/etd/266.

68. Li Z, Lee H, and Zhu C. Molecular mechanisms of mechanotransduction in integrin-mediated cellmatrix adhesion. *Exp Cell Res* (2016), **349**(1): 85-94.
69. Case BL, Baird MA, Shtengel G., Campbell SL, Hess HF, Davidson MW, and Waterman CM. Molecular mechanism of vinculin activation and nanoscale spatial organization in focal adhesions. *Nature Cell Biology* (2015), **17**(7): 880-892. doi:10.1038/ncb3180.
70. Riss TL, Moravec RA, Niles AL, et al. Cell Viability Assays. In: *Sittampalam GS, Coussens NP, Brimacombe K, et al., editors. Assay Guidance Manual [Internet]*. Bethesda (MD): Eli Lilly & Company and the National Center for Advancing Translational Sciences, 2013 May 1 [Updated 2016 Jul 1]. Available from: https://www.ncbi.nlm.nih.gov/books/NBK144065/.
71. van Meerloo J, Kaspers GJL, and Cloos J. *Cell sensitivity assays: the MTT assay.* In: Cree IA. (eds) *Cancer cell culture: methods and protocols*. 2nd ed. Totowa: Humana Press, 2011. ISBN 978-1-61779-079-9.
72. Brånemark PI. *The Osseointegration Book – From Calvarium to Calcaneus*; Berlin: Quintessence, 2005. ISBN 9781850970903. p. 24.
73. Albrektsson T, and Zarb G. The long-term efficacy of currently used dental implants: a review and proposed criteria of success. *Int J Oral Maxillofac Implants* (1986), **1**(1):11-25.
74. Parithimarkalaignan S, and Padmanabhan TV. Osseointegration: an update. *J Indian Prosthodont Soc.* (2013), **13**(1): 2–6.
75. Rahbek O., Overgaard S, Lind M, et al. The influence of hydroxyapatite coating on the peri-implant migration of polyethylene particles. *J Bone Joint Surg* (2001), **83-B**(3): 441-447.
76. Cordioli G, Majzoub Z, Piattelli A, and Scarano A. Removal torque and histomorphometric investigation of 4 different titanium surfaces: An experimental study in the rabbit tibia. *Int J Oral Maxillofac Implants* (2000), **15**(5): 668-674.
77. Piattelli M, Scarano A, Paolantonio M, et al. Bone response to machined and resorbable blast material titanium implants: An experimental study in rabbits. *J Oral Implantol* (2002), **28**(1): 2-8.
78. Khang W, Feldman S, Hawley CE, and Gunsolley J. A multi-center study comparing dual acid-etched and machined-surfaced implant in various bone

qualities. *J Periodontal* (2001), **72**(10): 1384-1390. DOI: 10.1902/jop.2001.72.10.1384.

79. Davarpanah M, Martinez H, Etienne D, et al. A prospective multicenter evaluation of 1,583 3i implants: 1- to 5-year data. *Int J Oral Maxillofac* Implants (2002), **17**(6): 820-828.
80. Trisi P, Lazzara R, Rao W, and Rebaudi A. Bone-implant contact and bone quality: Evaluation of expected and actual bone contact on machined an osseotite implant surfaces. *Int J Periodontics Restorative Dent* (2002), **22**(6): 535-545.
81. Trisi P, Lazzara R , Rebaudi A, et al. Bone-implant contact on machined and dual acid-etched surface after 2 months of healing in the human maxilla. *J Periodontal* (2003), **74**(7): 945-956. DOI: 10.1902/jop.2003.74.7.945.

6 Appendices

Appendix I

VACLAV BABUSKA, JANA DOBRA, VLASTIMIL KULDA, MICHAELA KRIPNEROVA, AMIN MOZTARZADEH, LUKAS BOLEK, JIRI LAHODA, DANIEL HRUSAK Comparison of fibroblast and osteoblast response to cultivation on titanium implants with different grain size. *Journal of Nanomaterials*, 2015, Article ID: 920893, 9 pages
DOI: 10.1155/2015/920893 [https://www.hindawi.com/journals/jnm/2015/920893/]

Appendix II

VACLAV BABUSKA, OMID MOZTARZADEH, TEREZA KUBIKOVA, AMIN MOZTARZADEH, DANIEL HRUSAK Evaluating the Osseointegration of Nanostructured Titanium Implants in Animal Models: Current Experimental Methods and Perspectives. *BIOINTERPHASES*, 2016, vol. 11, iss. 3, Article 030801, 11 pages
DOI: 10.1116/1.4958793 [http://avs.scitation.org/doi/abs/10.1116/1.4958793]

Appendix III

MOZTARZADEH AMIN, MOZTARZADEH OMID, KUBIKOVA TEREZA, TONAR ZBYNEK, HRUSAK DANIEL, ZICHA ANTONIN, BABUSKA VACLAV Současné metody hodnocení oseointegrace implantátů z nanostrukturního titanu (Current Methods for Assessing Osseointegration of Nanostructured Titanium Implants). *Chemické listy*, ***in press***